PNNL-25076
EMSP-RPT-033 Rev 0

Pacific Northwest
NATIONAL LABORATORY

Proudly Operated by **Battelle** *Since 1965*

Oxidative Stability of Tc(I) Tricarbonyl Species Relevant to the Hanford Tank Waste

SD Chatterjee
GB Hall
TG Levitskaia
ED Walter
NM Washton

December 2015

U.S. DEPARTMENT OF
ENERGY

Prepared for the U.S. Department of Energy
under Contract **DE-AC05-76RL01830**

PACIFIC NORTHWEST NATIONAL LABORATORY
operated by
BATTELLE
for the
UNITED STATES DEPARTMENT OF ENERGY
under Contract DE-AC05-76RL01830

Printed in the United States of America

Available to DOE and DOE contractors from the
Office of Scientific and Technical Information,
P.O. Box 62, Oak Ridge, TN 37831-0062;
ph: (865) 576-8401
fax: (865) 576-5728
email: reports@adonis.osti.gov

Available to the public from the National Technical Information Service
5301 Shawnee Rd., Alexandria, VA 22312
ph: (800) 553-NTIS (6847)
email: orders@ntis.gov <http://www.ntis.gov/about/form.aspx>
Online ordering: http://www.ntis.gov

PNNL-25076
EMSP-RPT-033 Rev 0

Oxidative Stability of Tc(I) Tricarbonyl Species Relevant to the Hanford Tank Waste

SD Chatterjee
GB Hall
TG Levitskaia
ED Walter
NM Washton

December 2015

Prepared for
the U.S. Department of Energy
under Contract DE-AC05-76RL01830

Pacific Northwest National Laboratory
Richland, Washington 99352

Summary

Technetium (Tc), which exists predominately in the liquid supernatant and salt cake fractions of the nuclear tank waste stored at the U.S. DOE Hanford Site, is one of the most difficult contaminants to dispose of and/or remediate. In the strongly alkaline environments prevalent in the tank waste, its dominant chemical form is pertechnetate (TcO_4^-, oxidation state +7). However, based on experimentation to-date, a significant fraction of the soluble Tc cannot be effectively separated from the wastes and may be present as a non-pertechnetate species. The presence of a non-pertechnetate species significantly complicates disposition of low-activity waste (LAW), and the development of methods to either convert them to pertechnetate or to separate the non-pertechnetate species directly is needed. The challenge is the uncertainty regarding the nature and stability of the alkaline-soluble, low-valence, non-pertechnetate species in the liquid tank waste. One objective of the Tc management project is to address this knowledge gap.

This fiscal year (FY) 2015 report summarizes experimental work exploring the oxidative stability of model low-valence Tc(I) tricarbonyl species, derived from the $[Tc(CO)_3]^+$ moiety. These compounds are of interest due to their implied presence in several Hanford tank waste supernatants. Work in part was initiated in FY 2014, and a series of samples containing non-pertechnetate Tc generated *ex situ* or *in situ* in pseudo-Hanford tank supernatant simulant solutions was prepared and monitored for oxidation to Tc(VII) (Levitskaia et al. 2014). This experimentation continued in FY 2015, and new series of samples containing Tc(I) as $[Tc(CO)_3]^+$•Ligand was tested. The monitoring method used for these studies was a combination of ^{99}Tc NMR and EPR spectroscopies.

The major achievement of this work is the development of stable non-pertechnetate Tc resistant to oxidation to Tc(VII) in a pseudo-Hanford tank supernatant simulant. The key findings are summarized below.

- ***Stable non-pertechnetate species were generated ex situ*** by a laboratory synthetic route ***include Tc(I) $[Tc(CO)_3]^+$•IDA complex*** **(where IDA is iminodiacetate),** which accounted for about 70% of total Tc present in the sample 4 months after sample preparation. The oxidation rate of the $[Tc(CO)_3]^+$•Gluconate complex was considerably faster than the tricarbonyl-IDA complex, and Tc(I)-gluconate species completely oxidized to $Tc(VII)O_4^-$ in 65 – 70 days. Complex $[Tc(CO)_3]^+$•Ligand species, where ligand is a polyaminocarboxylate chelator, were found to easily oxidize to TcO_4^-.

- ***Stable non-pertechnetate species were generated in situ*** from TcO_4^- using CO/H_2 reductant at elevated pressure and temperature in pseudo-Hanford tank supernatant simulant with and without gluconate and/or catalytic noble metals. Interestingly, stable non-pertechnetate products included both Tc(I) $[Tc(CO)_3]^+$-based species as well as Tc(II/IV/VI) species in intermediate oxidation states. The nature of these intermediate Tc oxidation species was largely dependent on the presence of the catalytic noble metals in the simulant, which promoted formation of the $[Tc(CO)_3]^+$ reduction products. With time $[Tc(CO)_3]^+$ either converted to other non-pertechnetate species or oxidized to TcO_4^-. Intriguingly, Tc(II/IV/VI) non-pertechnetate species in the intermediate oxidation states was found to be exceptionally resistant to further oxidation. Overall, significant fractions of *in situ* generated non-pertechnetate persisted in three out of four

simulant samples. To our knowledge this is the first identification of alkaline-stable inorganic Tc(II, IV and/or VI) species in intermediate oxidation states, and additional experimentation is warranted for elucidation of their structure and chemical composition.

A significant discovery of this work is that stability of non-pertechnetate in the Hanford tank supernatants may potentially be explained by inter-conversion among Tc species in various oxidation states. The finding that small organic chelators (e.g., iminodiacetate or gluconate) can stabilize Tc(VI) in the supernatants for prolonged times is significant, in particular because this Tc oxidation state is usually regarded as highly unstable. This also can be accentuated by lack of the analytical methods to quantify and characterize Tc in intermediate oxidation states, e.g., Tc(II and VI). To this end, development of the EPR method is critical to the actual tanks waste analysis.

Results of this task emphasize that considerable work remains, specifically to achieve control over Tc redox behavior in the alkaline media, and to develop methods for the separation of non-pertechnetate species from LAW by either their conversion to pertechnetate or direct removal. ***Examination of Tc speciation in actual waste samples collected from various Hanford tanks and evaluating the feasibility of treatment of total Tc is integral for the development of successful waste processing strategies.***

Acknowledgements

This work was completed as part of the Technetium Management Hanford Site project. Support for this project came from the U.S. Department of Energy's Office of Environmental Management. We would like to especially acknowledge the support of Dr. Nicholas Machara.

The authors would like to thank RJ Serne for his technical review.

Acronyms and Abbreviations

DIW	deionized water
DST	double shell tank
DTPA	diethylenetriamine pentaacetic acid
EDTA	ethylenediaminetetraacetic acid
EPR	electron paramagnetic resonance
FY	fiscal year
IDA	iminodiacetic acid
LAW	low-activity waste
LSC	liquid scintillation counting
NMR	nuclear magnetic resonance
NTA	nitrilotriacetic acid
PEP	Pretreatment Engineering Platform
PNNL	Pacific Northwest National Laboratory
QA	Quality Assurance
RPL	Radiochemical Processing Laboratory
SST	single shell tank
UV-Vis	ultraviolet-visible

Contents

Figures

Tables

1.0 Introduction

Technetium (Tc), which exists predominately in the liquid supernatant and salt cake fractions of the nuclear tank waste stored at the U.S. DOE Hanford Site, is one of the most difficult contaminants to dispose of and/or remediate. In strongly alkaline environments, Tc exists as pertechnetate (TcO_4^-) (oxidation state VII) and in the reduced forms (oxidation state < VII) collectively known as non-pertechnetate (non-TcO_4^-) species. Pertechnetate is a well-characterized, anionic Tc species that can be removed from LAW by anion exchange or other methods (Duncan et al. 2011). There is no definitive information on the origin or comprehensive description of the non-TcO_4^- species in Hanford tanks. This project is focused on characterization of the composition of non-TcO_4^- species to gain better understanding and control over their redox behavior. The objective of this work is to investigate interconversion among soluble TcO_4^- and soluble non-TcO_4^- species and to elucidate the mechanistic pathways for the separation of non-TcO_4^- species from LAW.

In fiscal year 2012 (FY 2012), a study reviewed prior work on the nature and extent of this non-pertechnetate, alkaline-soluble technetium in the Hanford waste tanks (Rapko et al. 2013a). As noted in that report, prior work has tentatively identified a Tc(I) carbonyl type compound as a non-pertechnetate species present in tank waste. In FY 2013, laboratory research began to investigate the chemistry of the Tc-tricarbonyl compound noted above. Multiple synthetic approaches described in the literature to prepare compounds with this structural feature were explored. A method was selected which, albeit time-consuming, was shown to provide a Tc-tricarbonyl compound pure with respect to Tc. Characterization of this product by a variety of methods was also explored and a report summarizing the FY 2013 work was issued (Rapko et al. 2013b). In FY 2014-2015, the optimization of the synthesis and purification of the Tc-tricarbonyl starting precursor was completed (Levitskaia et al. 2014; Hall et al. 2015). The experimental work continued on understanding various aspects of the nature and stability of various Tc-tricarbonyl species under simple alkaline conditions, alkaline conditions in the presence of the complexing agent sodium gluconate, high-ionic-strength alkaline conditions in the presence and absence of gluconate, and in the presence of alkaline Hanford tank solution simulants (Levitskaia et al. 2014; Levitskaia et al. 2015). It was found that high ionic strength solutions typifying Hanford tank waste supernatants promote oxidative stability of the *fac*-$[Tc(CO)_3]^+$ species[1]. The proof-of-principle tests were conducted to evaluate the concept of reductive conversion of pertechnetate to Tc-tricarbonyl in the simulant solutions (Levitskaia et al. 2014).

This report describes FY 2015 research activities focusing on the evaluation of the nature and oxidative stability of non-pertechnetate species relevant to the Hanford tank waste supernatants. Work was in part initiated in FY 2014, and a series of samples containing non-pertechnetate Tc generated *ex situ* or *in situ* in pseudo-Hanford tank supernatant simulant solutions.[2] After being prepared the non-pertechnetate species were monitored for re-oxidation to Tc(VII). This monitoring continued in FY 2015. In addition, a new series of samples containing Tc(I) as $[Tc(CO)_3]^+$•Ligand (where Ligand is a small organic chelator) was tested for oxidative stability.

[1] All Tc(I) carbonyl compounds described in this report have *facial* octahedral geometry, and in the following text the notation “*fac*-“ is omitted for clarity.

[2] In the context of this work, *ex situ* and *in situ* generation of the non-pertechnetate species is referred to their preparation by reduction of Tc(VII) using synthetic route followed by addition to the test solution (*ex situ*) as opposed to the Tc(VII) reduction directly in the test solution (*in situ*).

2.0 Quality Assurance

This work was conducted as part of Pacific Northwest National Laboratory (PNNL) Project 54042 under the Technetium Management Program, with funding from the U.S. Department of Energy Office of Environmental Management.

All research and development (R&D) work at PNNL is performed in accordance with PNNL's laboratory-level Quality Management Program, which is based on a graded application of NQA-1-2000, *Quality Assurance Requirements for Nuclear Facility Applications*, to R&D activities. In addition to the PNNL-wide quality assurance (QA) controls, the QA controls of the WRPS Waste Form Testing Program (WWFTP) QA program were also implemented for the work. The WWFTP QA program consists of the WWFTP Quality Assurance Plan (QA-WWFTP-001) and associated QA-NSLW-numbered procedures that provide detailed instructions for implementing NQA-1 requirements for R&D work. The WWFTP QA program is based on the requirements of NQA-1-2008, *Quality Assurance Requirements for Nuclear Facility Applications*, and NQA-1a-2009, *Addenda to ASME NQA-1-2008 Quality Assurance Requirements for Nuclear Facility Applications*, graded on the approach presented in NQA-1-2008, Part IV, Subpart 4.2, "Guidance on Graded Application of Quality Assurance (QA) for Nuclear-Related Research and Development". Preparation of this report and performance of the associated experimental work were assigned the technology level "Applied Research" and were conducted in accordance with procedure QA-NSLW-1102, *Scientific Investigation for Applied Research*. All staff members contributing to the work have technical expertise in the subject matter and received QA training prior to performing quality-affecting work. The "Applied Research" technology level provides adequate controls to ensure that the activities were performed correctly. Use of both the PNNL-wide and WWFTP QA controls ensured that all client QA expectations were addressed in performing the work.

3.0 Experimental

3.1 Materials

In-house NH_4TcO_4 stock solution available at the Radiochemical Processing Laboratory (RPL) at PNNL was used. Diglyme, acetonitrile, diethyl ether, dichloromethane, and borane-tetrahydrofuran BH_3/THF complex were obtained from Sigma-Aldrich and used without further purification. Gaseous CO and argon used in the diglyme synthesis of the $(Et_4N)_2[Tc(CO)_3Cl_3]$ were obtained from Matheson Tri-Gas. Inorganic sodium salts and aluminum nitrate were obtained from Sigma-Aldrich and were of reagent grade. All aqueous solutions were prepared from distilled water deionized to $\geq$15 MΩ cm with a Barnstead Nanopure water purification system.

Caustic solution simulating Hanford tank waste supernatants was prepared following a procedure previously developed for the Pretreatment Engineering Platform (PEP) testing (Scheele et al. 2009), albeit with a reduced NaOH concentration. The composition of the simulant is given in Table 1.

Table 1. PEP Supernatant Simulant Composition (Levitskaia et al. 2014)

Constituent	Concentration	
	µg/mL	M
Al^{3+}	5,900	0.217
Na^+	108,700	4.73
$C_2O_4^{2-}$	<450	<0.005
NO_2^-	25,300	0.55
NO_3^-	104,800	1.69
PO_4^{3-}	15,100	0.158
SO_4^{2-}	19,200	0.200
CO_3^{2-}	7,360	0.613
OH^-	18,800	0.47

3.2 Characterization Techniques

Technetium-99 nuclear magnetic resonance (NMR) spectroscopy. The NMR sample solutions were placed in capped polytetrafluoroethylene/fluorinated ethylene propylene copolymer sleeves (Wilmad Lab Glass, Vineland, NJ), which were then inserted into 5- or 10-mm glass NMR tubes to provide secondary containment for the radioactive liquid. ^{99}Tc NMR data were routinely collected at 67.565 MHz on a Tecmag Discovery spectrometer equipped with a 10-mm broadband Nalorac probe as described elsewhere (Cho et al. 2004) at the RPL at PNNL. A solution containing 10 mM TcO_4^- was used as a ^{99}Tc chemical shift reference, and all chemical shift data are quoted relative to TcO_4^- (Franklin et al. 1982).

Technetium-99 electron paramagnetic resonance (EPR) spectroscopy. EPR spectra were acquired on a Bruker EMX Spectrometer equipped with an ER4102ST resonator (spectra at room temperature and 120 K) or on an ER4116DM Dual Mode resonator (spectra at 5 K) and an Oxford ESR910 cryostat. Samples were doubly contained by employing unbreakable FEP tube liners (Wilmad) inside traditional quartz EPR tubes. Liquid samples employed 1.5 mm inner diameter (ID) liners and 4 mm outer diameter (OD) quartz tubes while frozen solution and powder samples used 3.15 mm ID liners and 5 mm OD tubes. The spectra were collected at a temperature of 125 ± 2 K.

Ultraviolet-visible (UV-vis) spectroscopy. UV spectrophotometric measurements were performed using a deuterium light source DH2000 MIKROPACK UV-VIS, grating No 1 with 100 µm slit width and a USB-2000 spectrophotometer 200-950 nm. Visible spectrophotometric measurements were acquired using an HL-2000 Tungsten Halogen Light Source and the same spectrometer. Three replicate measurements were collected for each location. Spectral data were processed using a SpectraSuite Spectroscopy Platform Software version 2.0.140 (Ocean Optics, Inc.).

Liquid Scintillation Counting (LSC). The concentration of Tc in the liquid samples was measured by a LSC technique. Typically, 10 mL of Ultima Gold XR liquid scintillation cocktail (Packard BioScience, Meriden, CT) was used for ^{99}Tc beta counting. The relative beta activity of the samples was determined using a Packard Tri-Carb Model 2500TR Liquid Scintillation Analyzer (Packard Instrument Company, Meriden, CT 06450) with a 0.98 counting efficiency. In a typical measurement, beta counts were integrated over a 10 min collection time; all counts were corrected for background and then converted to activity (or mass) by dividing by the stated efficiency.

3.3 Sample Preparation

Work on evaluating the stability of the aqua species of the general formula $[Tc(CO)_3(H_2O)_{3-n}(OH)_n]^{1-n}$ ($n = 0 – 3$) complexes in 0.5 – 5 M $NaNO_3$ / 0 – 2 M NaOH aqueous solutions had been initiated in FY 2014. The $[Tc(CO)_3(H_2O)_{3-n}(OH)_n]^{1-n}$ and $[Tc(CO)_3(OH)]_4$ compounds were obtained by dissolving $(Et_4N)_2[Tc(CO)_3Cl_3]$ precursor in 5 M $NaNO_3$ containing variable NaOH concentrations or simulant solution as described in our previous report (Levitskaia et al. 2014).

To monitor the oxidative stability of $[Tc(CO)_3]^+$ complexes with small organic chelators found in the Hanford tanks, these compounds were prepared using similar procedure. In the general procedure, $[Tc(CO)_3(OH)]_4$ was first converted to $[Tc(CO)_3(H_2O)_3]^+$ by dissolution in 1 M triflic acid, extraction into diethyl ether, and crystallization. Solid $[Tc(CO)_3(H_2O)_3]^+$ was dissolved in 5 M $NaNO_3$ / 0.1 M NaOH or in PEP/tank supernate simulant and mixed with the 0.2 M chelator solution in the same matrix in a 1:1 ratio so that the resulting solution contained 2.55 – 3.15 mM Tc(I) and 0.1 M chelator. The kinetic stability of the resulting $[Tc(CO)_3]^+$•Ligand complexes was monitored by ^{99}Tc NMR spectroscopy. The tested chelators included iminodiacetic acid (IDA), nitrilotriacetic acid (NTA), ethylenediaminetetraacetic acid (EDTA), and diethylenetriamine-N,N,N,N'',N''-pentaacetic acid (DTPA). The molecular structures of these compounds are shown in Figure 1.

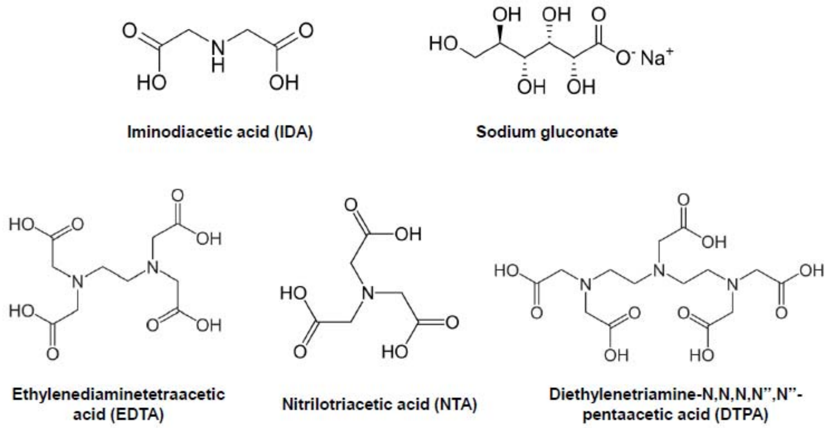

Figure 1. Molecular Structure of the Small Organic Chelators Used in This Study

Chemical reduction of TcO_4^- was attempted to study the reductive stability of pertechnetate and the potential for generation of non-pertechnetate $[Tc(CO)_3]^+$ or other intermediate species in the pseudo-Hanford tank supernatant simulant of composition given in Table 1. The reduction was carried out under four different reaction conditions using 10 mM NH_4TcO_4 solution in the simulant.

a) Parr reaction in presence of gluconate and noble metals:

Under the first condition, noble metals, including 0.13 mM Pt, 0.57 mM Pd, 0.014 mM Rh, and 1.04 mM Ru, were added to the simulant to simulate fission products. The 1 mM concentration of the noble metals was utilized in the previous work (Bernard et al. 2001), but was not achievable for Pt, Pd, and Rh due to their limited solubility in the simulant solution. The simulant was also adjusted to contain 0.10 M sodium gluconate to simulate complexant concentrations in Hanford DST tanks. ^{99}Tc NMR of the resulting solution exhibited a single resonance at -1 ppm showing TcO_4^- as the only observed NMR active Tc species. The solution was placed in an unstirred pressure vessel, flushed with CO, and pressurized with CO gas that contained approximately 75 ppm H_2. Subsequently, the solution was kept at 80 °C and 1300 psi for 10 days.

Three control reactions were carried out to identify and isolate the influences of the noble metals and gluconate as described below in b), c), and d).

b) Parr reaction in presence of noble metals with the exclusion of gluconate:

In the first control experiment gluconate was excluded from the synthesis and only noble metals (0.13 mM Pt, 0.57 mM Pd, 0.014 mM Rh, and 1.04 mM Ru) were added to the simulant. ^{99}Tc NMR of the resulting solution exhibited a single resonance at -1 ppm showing TcO_4^- as the only observed NMR active Tc species. The solution was placed in the unstirred pressure vessel, flushed with CO, and pressurized with CO gas that contained approximately 75 ppm H_2. Subsequently, the solution was kept at 80 °C and 1300 psi for 10 days.

c) Parr reaction in absence of noble metals with the inclusion of gluconate:

In the second control experiment, noble metals were excluded from the synthesis. The simulant was adjusted to contain 0.10 M sodium gluconate. ^{99}Tc NMR of the resulting solution exhibited a single resonance at about 0 ppm showing TcO_4^- as the only observed NMR active Tc species. Depending on the experimental conditions such as solution composition and temperature, the position of the NMR resonance for TcO_4^- fluctuates in the approximate range of – 10 to + 10 ppm (Cho et al. 2004). The solution was placed in the unstirred pressure vessel, flushed with CO, and pressurized with CO gas that contained approximately 75 ppm H_2. Subsequently, the solution was kept at 80 °C and 1300 psi for 7 days.

d) Parr reaction in the absence of both gluconate and noble metals:

In the third control experiment, neither noble metals nor gluconate were added to the simulant solution. ^{99}Tc NMR of the resulting solution exhibited a single resonance at 0 ppm showing TcO_4^- as the only observed NMR active Tc species. The solution was placed in an unstirred pressure vessel, flushed with CO, and pressurized with CO gas that contained approximately 75 ppm H_2. Subsequently, the solution was kept at 80 °C and 1300 psi for 10 days.

Upon conclusion of each of the tests, the solution was returned to room temperature and atmospheric pressure, unsealed, and sampled soon after exposure to atmospheric conditions. Liquid fractions of the reaction mixtures were withdrawn and analyzed by LSC, ^{99}Tc NMR and EPR. Samples were periodically monitored by ^{99}Tc NMR for about 1 year, during monitoring all Tc samples were stored under ambient laboratory conditions and were not protected from exposure to light.

4.0 Results and Discussion

4.1 Oxidative Stability of Generated *ex situ* $[Tc(CO)_3]^+$ Species

4.1.1 Continuation of the Studies Initiated in FY 2014

4.1.1.1 $[Tc(CO)_3(H_2O)_{3-n}(OH)_n]^{1-n}$ Aqua Species in Concentrated $NaNO_3$ Solutions

Studies evaluating oxidative stability of $[Tc(CO)_3(H_2O)_{3-n}(OH)_n]^{1-n}$ species in $NaNO_3$ / NaOH solutions were initiated in FY 2014 as described previously (Levitskaia et al. 2014). In these tests, $(Et_4N)_2[Tc(CO)_3Cl_3]$ was used to generate $[Tc(CO)_3(H_2O)_{3-n}(OH)_n]^{1-n}$ samples. The stability of aqueous Tc(I) coordination compounds over time with respect to their re-oxidation to TcO_4^- was monitored by ^{99}Tc NMR spectroscopy. This testing was continued in FY 2015 and is currently in progress for the high-stability Tc(I)-tricarbonyl solutions. The obtained results are shown in Tables 2 and 3.

^{99}Tc NMR measurements indicate that the $[Tc(CO)_3(H_2O)_{3-n}(OH)_n]^{1-n}$ species in near-neutral solutions containing 2, 5, or 5.7 M $NaNO_3$, show minimal oxidation to TcO_4^- within the time period of monitoring as evident from the absence of the corresponding Tc resonance around 0 ppm (Table 2). The 2 M $NaNO_3$ solution initially exhibited a single resonance at -868 ppm assigned to the $[Tc(CO)_3(H_2O)_3]^+$ specie, indicating a single Tc coordination environment. From day 3 onwards, $[Tc(CO)_3(H_2O)_3]^+$ started to convert to the tetrameric $[Tc(CO)_3(OH)]_4$ species as indicated by the appearance of a new resonance at -585 ppm corresponding to the tetramer. After conversion of about 60% of $[Tc(CO)_3(H_2O)_3]^+$ to $[Tc(CO)_3(OH)]_4$, the $[Tc(CO)_3]^+$ species seemed to reach a dynamic equilibrium. It should be noted that $[Tc(CO)_3]^+$ compounds were predominant even after 450 days of monitoring, with a tiny resonance due to TcO_4^- appearing on the 576th day of monitoring and amounting to <0.5% of total Tc concentration.

On the other hand, dissolution of $[Tc(CO)_3Cl_3]^{2-}$ in 5 or 5.7 M $NaNO_3$ solution resulted a mixture of both $[Tc(CO)_3(H_2O)_3]^+$ and $[Tc(CO)_3(OH)]_4$ species. With time, gradual conversion of $[Tc(CO)_3(H_2O)_3]^+$ to $[Tc(CO)_3(OH)]_4$ was observed, this process was completed in 75 – 80 days. It is known that at near-neutral pH, the $[Tc(CO)_3(H_2O)_3]^+$ complex undergoes partial hydrolysis and oligomerization to generate a tetrameric hydrolysis product $[Tc(CO)_3(OH)]_4$ (Alberto et al. 1998; Gorshkov et al. 2000). The formation of the $[Tc(CO)_3(OH)]_4$ tetramer primarily depends on the solution pH and Tc(I) concentration. In 5 and 5.7 M $NaNO_3$ solutions, the concentration of Tc(I) was about 7 times greater than in 2 M $NaNO_3$ solution, which undoubtedly led to the enhanced formation of the $[Tc(CO)_3(OH)]_4$ species. In 5 and 5.7 M $NaNO_3$ solutions, less than 0.5% of TcO_4^- was observed after 154 and 132 days of monitoring respectively. However, it is worth mentioning that there was no further increase in TcO_4^- even after 564 and 563 days of monitoring, respectively.

Table 2. Time Stability of $[Tc(CO)_3]^+$ Species in $NaNO_3$ Solutions Monitored by ^{99}Tc NMR Spectroscopy. Relative quantities of the Tc(I) species $[Tc(CO)_3(H_2O)_3]^+$ and $[Tc(CO)_3(OH)]_4$ were determined by the integration of the corresponding resonances at about -868 and -585 ppm, respectively.

Time Elapsed	**Percent Fraction**			
	$[Tc(CO)_3(H_2O)_3]^+$	**$[Tc(CO)_3(OH)]_4$**	**total non-TcO_4^-**	**TcO_4^-**
2 M $NaNO_3$ / 0.028 mM Tc				
Start Day	1	0	1	0
1 day	1	0	1	0
2 days	1	0	1	0
3 days	0.95	0.05	1	0
4 days	0.92	0.08	1	0
7 days	0.84	0.16	1	0
8 days	0.82	0.18	1	0
10 days	0.80	0.20	1	0
18 days	0.73	0.27	1	0
25 days	0.65	0.35	1	0
45 days	0.62	0.38	1	0
86 days	0.61	0.39	1	0
125 days	0.63	0.37	1	0
163 days	0.65	0.35	1	0
209 days	0.66	0.34	1	0
296 days	0.68	0.32	1	0
576 days	0.70	0.30	>0.995	<0.005
5 M $NaNO_3$ / 0.19 mM Tc				
Start Day	0.51	0.49	1	0
3 days	0.28	0.72	1	0
3 days	0.19	0.81	1	0
11 days	0.08	0.92	1	0
18 days	0.07	0.93	1	0
38 days	0.05	0.95	1	0
81 days	0.05	0.95	1	0
120 days	0.04	0.96	1	0
154 days	0.04	>0.955	>0.995	<0.005
193 days	0.04	>0.955	>0.995	<0.005
564 days	0.04	0.96	>0.995	<0.005
5.7 M $NaNO_3$ / 0.21 mM Tc				
Start Day	0.58	0.42	1	0

2 days	0.08	0.92	1	0
9 days	0	1	1	0
17 days	0	1	1	0
39 days	0	1	1	0
77 days	0	1	1	0
132 days	0	>0.995	>0.995	<0.005
159 days	0	>0.995	>0.995	<0.005
194 days	0	>0.995	>0.995	<0.005
563 days	0	>0.995	>0.995	<0.005

Among alkaline solutions (0.01 – 2 M NaOH) with high nitrate concentrations (5 M $NaNO_3$) prepared in FY 2014, Tc(I) had fully oxidized to Tc(VII) by the end of FY 2014 in all solutions but the 5 M $NaNO_3$/0.01 M NaOH (Levitskaia et al. 2014). Monitoring of this sample has been continued in FY 2015 and the results are summarized in Table 3. Due to the high pH (about 13) of this solution, the NMR spectrum exhibited a single resonance at -1070 ppm corresponding to the mono-deprotonated $[Tc(CO)_3(H_2O)_2(OH)]$ monomeric species. It is interesting to note that initially a simple oxidative decomposition of $[Tc(CO)_3(H_2O)_2(OH)]$ to TcO_4^- was observed initially for a period of 74 days. This was followed by combination of two gradual processes, oligomerization of $[Tc(CO)_3(H_2O)_2(OH)]$ monomer to the $[Tc(CO)_3(OH)]_4$ tetramer and oxidative decomposition of the $[Tc(CO)_3]^+$ species to TcO_4^-. This finding is consistent with the previous reports (Alberto et al. 1998 and references therein) showing the formation of tetrameric species depends of the Tc concentration and solution pH (Rapko et al. 2013b).

Table 3. Time Stability of $[Tc(CO)_3]^+$ Species in 5 M $NaNO_3$ / 0.1 M NaOH Solution , with 0.19 mM Tc Monitored by ^{99}Tc NMR Spectroscopy. Relative quantities of $[Tc(CO)_3(H_2O)_2(OH)]$, $[Tc(CO)_3(OH)]_4$ and TcO_4^- were determined by the integration of the corresponding resonances at -1070, -585, and near 0 ppm.

Time Elapsed	**Percent Fraction**			
	$[Tc(CO)_3(H_2O)_3(OH)]$	**$[Tc(CO)_3(OH)]_4$**	**Total non-TcO_4^-**	**TcO_4^-**
Start Day	1	0	1	0
1 day	1	0	1	0
2 days	1	0	1	0
10 days	1	0	1	0
16 days	0.95	0	0.95	0.05
37 days	0.90	0	0.90	0.1
78 days	0.90	0	0.90	0.1
117 days	0.79	0.06	0.85	0.15
158 days	0.61	0.11	0.72	0.28
196 days	0.60	0.15	0.61	0.39
563 days	0.03	0.42	0.45	0.55

4.1.1.2 Monitoring of $[Tc(CO)_3]^+$ Species in Simulant Solutions

In FY 2014, to test the stability of the $[Tc(CO)_3]^+$ species in a pseudo-Hanford tank supernatant simulant a series of samples was prepared by the direct dissolution of the $(Et_4N)_2[Tc(CO)_3Cl_3]$ compound in the simulant solution containing catalytic noble metals (0.13 mM Pt, 0.57 mM Pd, 0.014 mM Rh, and 1.04 mM Ru) with or without 0.05 M gluconate at variable pH (Levitskaia et al. 2014). The monitoring of these samples continued in FY 2015. The new results are summarized in Tables 4 and 5.

Table 4. Stability of $[Tc(CO)_3]^+$ Species in a Pseudo-Hanford Tank Supernatant Simulant Containing Noble Metals Monitored by ^{99}Tc NMR Spectroscopy as a Function of Time. Relative quantities of $[Tc(CO)_3(H_2O)_2(OH)]$ and TcO_4^- were determined by the integration of the corresponding resonances at -1070 and near 0 ppm.

Time Elapsed	Percent Fraction	
	$[Tc(CO)_3(H_2O)_2(OH)]$	**TcO_4^-**
0.47 M NaOH in simulant (total 5.2 M Na) / noble metals / 12.2 mM Tc		
Start Day	0.94	0.06
1 day	0.92	0.08
2 days	0.89	0.11
3 days	0.89	0.11
6 days	0.79	0.21
10 days	0.72	0.28
14 days	0.63	0.37
20 days	0.48	0.52
23 days	0.45	0.55
28 days	0.37	0.63
34 days	0.26	0.74
39 days	0.13	0.87
40 days	0.11	0.89
45 days	0.07	0.93
50 days	0	1
0.83 M NaOH in simulant (5.2 M Na) / noble metals / 12.2 mM Tc		
Start Day	0.96	0.04
1 day	0.89	0.11
3 days	0.78	0.22
8 days	0.55	0.45
12 days	0.39	0.61
16 days	0.21	0.79
19 days	0.16	0.84
24 days	0.11	0.89
29 days	0.07	0.93
32 days	0.03	0.97

35 days	0	1
1.47 M NaOH in simulant (total 5.7 M Na) / noble metals / 12.2 mM Tc		
Start Day	0.95	0.05
1 day	0.82	0.18
3 days	0.63	0.37
6 days	0.42	0.58
8 days	0.17	0.83
10 days	0	1

Table 5. Stability of $[Tc(CO)_3]^+$ Species in a Pseudo-Hanford Tank Supernatant Simulant Containing Noble Metals and Gluconate by ^{99}Tc NMR Spectroscopy as a Function of Time. Relative quantities of the $[Tc(CO)_3]^+$•Gluconate complex species and TcO_4^- were determined by the integration of the corresponding resonances at about -1232/-1254 (combined integration) and near 0 ppm.

Time Elapsed	**Percent Fraction**	
	$[Tc(CO)_3]^+$•Gluconate	**TcO_4^-**
0.47 M OH in simulant / 0.05 M gluconate / noble metals /13.7 mM Tc		
Start Day	0.87	0.13
1 day	0.70	0.30
2 days	0.68	0.32
3 days	0.62	0.38
6 days	0.48	0.52
10 days	0.42	0.58
16 days	0.39	0.61
22 days	0.34	0.66
29 days	0.29	0.71
37 days	0.25	0.75
43 days	0.21	0.79
66 days	0.09	0.91
78 days	0	1
0.47 M OH in simulant / 0.05 M gluconate / noble metals / 13.7 mM Tc / CO atmosphere		
Start Day	0.79	0.21
1 day	0.65	0.35
2 days	0.62	0.38
3 days	0.58	0.42
6 days	0.58	0.42
10 days	0.51	0.49
17 days	0.45	0.55
22 days	0.39	0.61

29 days	0.30	0.70
37 days	0.25	0.75
45 days	0.21	0.79
64 days	0.11	0.89
79 days	0	1

It was observed that [$Tc(CO)_3(H_2O)_2(OH)$] species in the simulant (composition given in Table 1) containing noble metals oxidized to Tc(VII) in 50 days (Table 4). Consistent with our previous observations, the kinetics of [$Tc(CO)_3$ $(H_2O)_2(OH)$] oxidation in this simulant is significantly slower than in the 5 M $NaNO_3$ / 0.5 M NaOH solution in which oxidation was complete in 10 days (Levitskaia et al. 2014). Increase of the hydroxide concentration to 0.83 and 1.47 M in the simulant containing noble metals resulted in concomitant decrease of the stability of [$Tc(CO)_3(H_2O)_2(OH)$], which is fully oxidized to Tc(VII) in 35 and 10 days, respectively.

Samples prepared in the simulant solution containing noble metals and gluconate, with one sample under a CO atmosphere, exhibited the formation of the $[Tc(CO)_3]^+$•Gluconate complex as evident from the Tc(I) resonances at -1232 and -1254 ppm. Both samples exhibited very similar behavior with $[Tc(CO)_3]^+$•Gluconate fully oxidized to Tc(VII) in about 78 – 79 days (Table 5). In comparison oxidation of the [$Tc(CO)_3(H_2O)_2(OH)$] species obtained in the same simulant without gluconate was completed in 50 days (Table 4). So it was concluded that the $[Tc(CO)_3]^+$•Gluconate complex is slightly more stable than the [$Tc(CO)_3(H_2O)_2(OH)$] species under tested experimental conditions.

4.1.2 $[Tc(CO)_3]^+$•Ligand Complexes: FY 2015 Studies

In FY 2015, Tc(I) complexes containing the $[Tc(CO)_3]^+$ moiety coordinated with IDA, gluconate, NTA, EDTA, or DTPA were prepared by dissolution of solid $[Tc(CO)_3(H_2O)_3]^+$ as described in Section 3.3 in either 5 M $NaNO_3$ / 0.1 M NaOH or simulant matrix and monitored by ^{99}Tc NMR spectroscopy. In all cases it was observed that [$Tc(CO)_3(H_2O)_2(OH)$] initially formed upon dissolution of the $[Tc(CO)_3(H_2O)_3]^+$ material in the alkaline solutions, which slowly converted to the $[Tc(CO)_3]^+$•Ligand complex. The efficiency of this conversion depends on the chelator affinity for the $[Tc(CO)_3]^+$ moiety and its ability to exchange water and hydroxide ligands in [$Tc(CO)_3(H_2O)_2(OH)$] specie. Both conversion of [$Tc(CO)_3(H_2O)_2(OH)$] to $[Tc(CO)_3]^+$•Ligand and their oxidation to Tc(VII) was monitored with time.

4.1.2.1 $[Tc(CO)_3]^+$•IDA

It was found that IDA exhibits strong coordination affinity toward $[Tc(CO)_3]^+$ both in 5 M $NaNO_3$ / 0.1 M NaOH and simulant solutions. The obtained results are summarized in Table 6 and some representative spectra are shown in Figure 2. Within ~15 minutes of the preparation of solution containing [$Tc(CO)_3(H_2O)_2(OH)$] and IDA in 5 M $NaNO_3$ / 0.1 M NaOH matrix, NMR monitoring showed a significant decrease in the intensity of the [$Tc(CO)_3(H_2O)_2(OH)$] resonance, coupled with the appearance of a strong broad resonance at about -1000 ppm (Figure 2) and a weak broad resonance at -850 ppm (Figure 3), both assigned to $[Tc(CO)_3]^+$•IDA complexes. About 80% and 92% of the total Tc(I) was converted to the complexed $[Tc(CO)_3]^+$•IDA form in 1 and 24 hours post sample preparation, respectively (Table 6). In the simulant, the kinetics of complexation was slightly slower, with ~ 40 and 90% of Tc(I) converted to $[Tc(CO)_3]^+$•IDA within the first hour and two days, respectively.

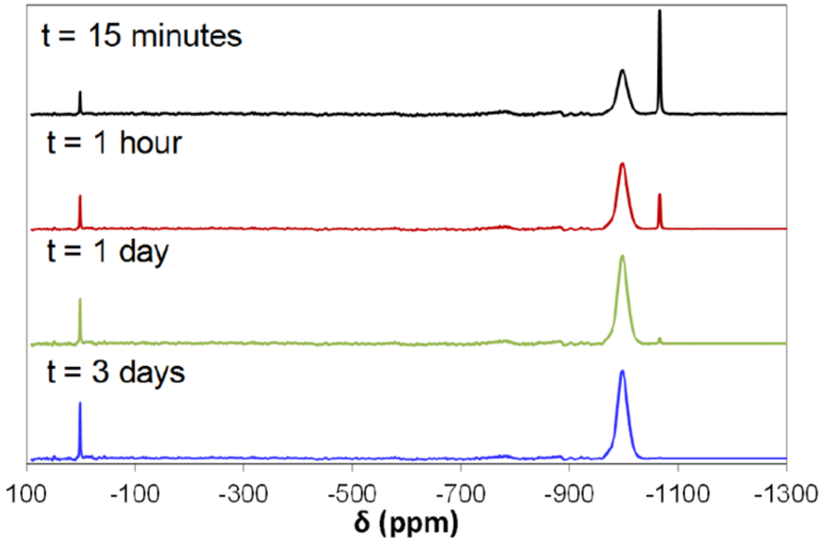

Figure 2. Monitoring the Kinetics of Complexation of $[Tc(CO)_3(H_2O)_2(OH)]$ with IDA in 5 M $NaNO_3$ / 0.1 M NaOH Using Solution ^{99}Tc NMR Spectroscopy: the Entire Spectral Region. The resonances at 0 and -1065 ppm correspond to TcO_4^- and $[Tc(CO)_3(H_2O)_2(OH)]$, while two resonances at -1000 and -850 ppm are assigned to $[Tc(CO)_3]^+$•IDA.

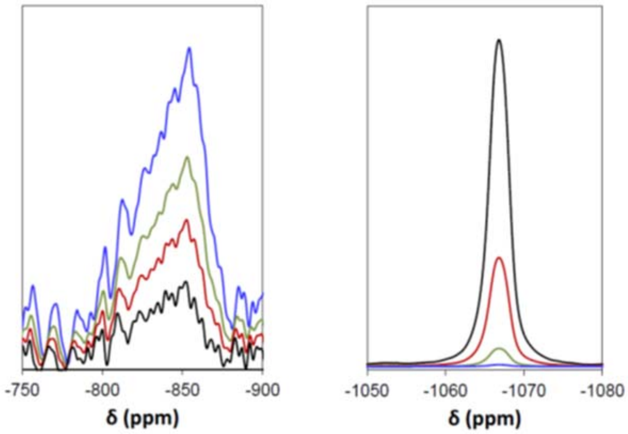

Figure 3. Monitoring the Kinetics of Complexation of $[Tc(CO)_3(H_2O)_2(OH)]$ with IDA in 5 M $NaNO_3$ / 0.1 M NaOH Using Solution ^{99}Tc NMR Spectroscopy: the -850 ppm and -1065 ppm Spectral Regions (the entire spectra are shown in Figure 2). Left panel: bottom black trace: 15 minutes, second from bottom red trace: 1 hour, second from top green trace: 1 day, top blue trace: 5 days. Right panel: top black trace: 15 minutes, second from top red trace: 1 hour, second from bottom green trace: 1 day, bottom blue trace: 5 days.

NMR monitoring of the $[Tc(CO)_3]^+$•IDA species indicated their remarkable stability with respect to oxidative decomposition (Figure 4), so that ~25 and 30% of Tc(I) oxidized to TcO_4^- in 5 M $NaNO_3$ / 0.1 M NaOH solution in 4.5 months and in the simulant solution in 4 months, respectively

(Table 6). The initial formation of TcO_4^- during the first few days post sample preparation was speculatively attributed to the decomposition of the unstable $[Tc(CO)_3(H_2O)_2(OH)]$ compound.

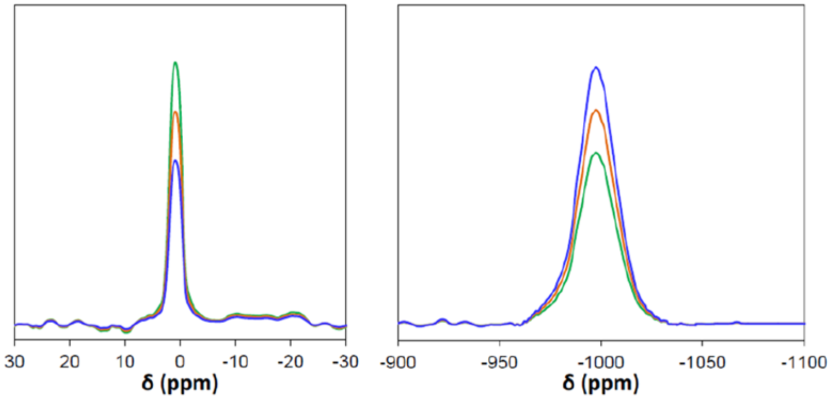

Figure 4. Comparison of the ^{99}Tc NMR Spectra of the $[Tc(CO)_3]^+$•IDA Species in 5 M $NaNO_3$ / 0.1 M NaOH Solution with Time. Left panel: TcO_4^- region (0 ppm); bottom blue trace: t = 3 days, middle orange trace: t = 40 days, top green trace: t = 132 days. Right panel: $[Tc(CO)_3]^+$•IDA region (-1000 ppm); top blue trace: t = 3 days, middle orange trace: t = 40 days, bottom green trace: t = 132 days.

Table 6. Formation Kinetics and Oxidative Stability of the $[Tc(CO)_3]^+$•IDA Complex in 5 M $NaNO_3$ / 0.1 M NaOH and Simulant Solutions Monitored by ^{99}Tc NMR Spectroscopy. Relative quantities of $[Tc(CO)_3(H_2O)_2(OH)]$, $[Tc(CO)_3]^+$•IDA, and TcO_4^- were determined by the integration of the corresponding resonances at -1065, -1000 and near 0 ppm, respectively.

Time Elapsed	Percent Fraction		
	$[Tc(CO)_3(H_2O)_2(OH)]$	**$[Tc(CO)_3]^+$•IDA**	**TcO_4^-**
5 M $NaNO_3$ / 0.1 M NaOH / 0.1 M IDA / 3.2 mM Tc			
0.2 hours	0.39	0.58	0.03
1 hour	0.18	0.78	0.03
1 day	0.04	0.92	0.04
5 day	0.02	0.94	0.04
10 days	0.01	0.93	0.06
15 days	0.01	0.92	0.08
20 days	0.00	0.92	0.08
25 days	0.00	0.91	0.09
31 days	0	0.90	0.11
40 day	0	0.88	0.12
53 days	0	0.86	0.14
66 days	0	0.85	0.15
81 days	0	0.82	0.18
96 days	0	0.80	0.20
114 days	0	0.78	0.22
132 day	0	0.75	0.25
0.47 M OH in simulant / 0.1 M IDA / 2.6 mM Tc			
Start Day	0.58	0.38	0.03
2 day	0.06	0.90	0.04
6 days	0.01	0.94	0.05
10 days	0.01	0.94	0.06
14 days	0.00	0.93	0.07
20 days	0.00	0.92	0.08
26 days	0	0.91	0.09
32 day	0	0.90	0.10
40 days	0	0.88	0.12
52 days	0	0.86	0.14
66 days	0	0.83	0.17
81 days	0	0.80	0.20
96 days	0	0.77	0.23
108 days	0	0.73	0.27
120 days	0	0.70	0.30

Tc speciation diagrams in 5 M $NaNO_3$ / 0.1 M NaOH and simulant solution containing IDA are shown in Figure 5, which demonstrates fast initial ingrowth of the $[Tc(CO)_3]^+$•IDA complex concurring with the reduction of the $[Tc(CO)_3(H_2O)_2(OH)]$ fraction. This is followed by gradual nearly linear oxidative decomposition of the $[Tc(CO)_3]^+$•IDA complex and corresponding increase of TcO_4^-.

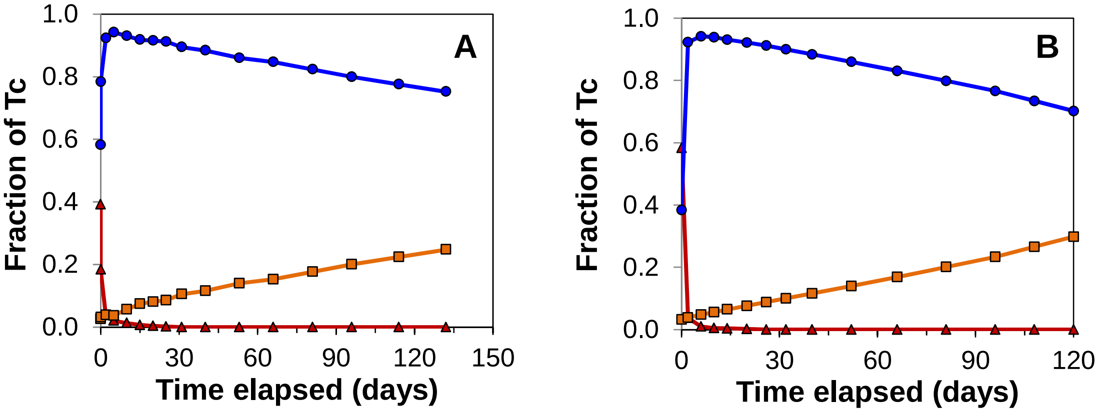

Figure 5. Tc Speciation Over Time During Reaction of $[Tc(CO)_3(H_2O)_2(OH)]$ with 0.1 M IDA in (A) 5 M $NaNO_3$ / 0.1 M NaOH and (B) Simulant. Top, blue circles: $[Tc(CO)_3]^+$•IDA. Bottom, red triangles: $[Tc(CO)_3(H_2O)_2(OH)]$. Middle, orange squares: TcO_4^-.

4.1.2.2 $[Tc(CO)_3]^+$•Gluconate

Gluconate has previously been observed to exhibit complexation of $[Tc(CO)_3]^+$ (Lukens et al. 2004; Rapko et al. 2013b) and stability of $[Tc(CO)_3]^+$•Gluconate was evaluated in our last year studies (Levitskaia et al. 2014). In this work, the stability of the $[Tc(CO)_3]^+$•Gluconate complex was monitored under conditions identical to those applied to other small chelator systems to generate comparable results. The obtained results are summarized in Table 7.

Table 7. Formation Kinetics and Oxidative Stability of the $[Tc(CO)_3]^+$•Gluconate Complex in 5 M $NaNO_3$ / 0.1 M NaOH and Simulant Solutions Monitored by ^{99}Tc NMR Spectroscopy. Relative quantities of $[Tc(CO)_3(H_2O)_2(OH)]$, $[Tc(CO)_3]^+$•Gluconate, and TcO_4^- were determined by the integration of the corresponding resonances at -1070, -1100/-1232/-1254 and near 0 ppm, respectively. The relative quantity of $[Tc(CO)_3]^+$•Gluconate was determined by the sum of the integrations of the resonances at -1100, -1232 and -1254 ppm.

Time Elapsed	**Percent Fraction**		
	$[Tc(CO)_3(H_2O)_2(OH)]$	**$[Tc(CO)_3]^+$•Gluconate**	**TcO_4^-**
5 M $NaNO_3$ / 0.1 M NaOH / 0.1 M gluconate / 3.2 mM Tc			
1.2 hours	0.98	0	0.03
1.8 hours	0.78	0.20	0.02
3 hours	0.58	0.40	0.02
1 day	0.09	0.88	0.04
2 days	0.06	0.80	0.14
4 days	0.04	0.72	0.25
6 days	0.02	0.62	0.36
12 days	0.01	0.52	0.47
18 days	0.00	0.42	0.58
24 days	0	0.31	0.69
32 days	0	0.24	0.76
40 days	0	0.18	0.82
48 days	0	0.10	0.90
60 days	0	0.02	0.98
72 days	0	0.01	1
0.47 M OH in simulant / 0.1 M gluconate / 2.6 mM Tc			
1.2 hours	0.99	0	0.02
1.8 hours	0.81	0.17	0.03
4 hours	0.63	0.33	0.04
1 day	0.19	0.78	0.03
2 days	0.08	0.79	0.12
4 days	0.04	0.80	0.16
8 days	0.03	0.71	0.27
12 days	0.01	0.61	0.37
18 days	0.00	0.52	0.48
24 days	0	0.42	0.58
32 days	0	0.33	0.67
40 days	0	0.24	0.77
48 days	0	0.14	0.86
55 days	0	0.05	0.95
64 days	0	0.01	1

The kinetics of the $[Tc(CO)_3(H_2O)_2(OH)]$ conversion to $[Tc(CO)_3]^+$•Gluconate was similar to that observed for IDA. The intensity of the $[Tc(CO)_3(H_2O)_2(OH)]$ NMR resonance gradually decreased, coupled with the ingrowth of broad resonances at -1232 and -1254 ppm and a very broad resonance at -1100 ppm. All three of these resonances are assigned to the $[Tc(CO)_3]^+$•Gluconate species suggesting three different $[Tc(CO)_3]^+$ chemical environments. After 3 hours of mixing, about 40% of the total Tc was converted to the gluconate complex. It is interesting to note that the rate of intensity increase for all the three resonances is equal. After 3 hours, the amount of gluconate complexed tri-carbonyl Tc(I) was observed to steadily increase, amounting to 78 – 88% complexation during the first day.

The stability of the $[Tc(CO)_3]^+$•Gluconate species were monitored by ^{99}Tc NMR spectroscopy, and the results are summarized in Table 7 and Figure 6. The $[Tc(CO)_3]^+$•Gluconate complex exhibited significantly lower stability with respect to oxidative decomposition to TcO_4^- compared to the $[Tc(CO)_3]^+$•IDA species. Near complete oxidation of $[Tc(CO)_3]^+$•Gluconate to Tc(VII) was observed in 72 and 64 days in 5 M $NaNO_3$ / 0.1 M NaOH and in simulant, respectively. Slightly faster decomposition in the simulant was attributed to the higher hydroxide concentration.

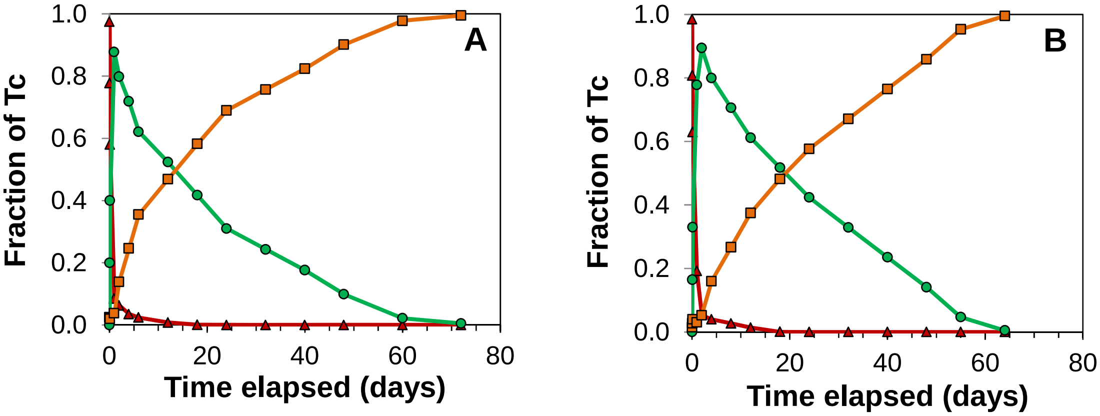

Figure 6. ^{99}Tc Time Speciation During Reaction of $[Tc(CO)_3(H_2O)_2(OH)]$ with 0.1 M Gluconate in (A) 5 M $NaNO_3$ / 0.1 M NaOH and (B) Simulant. Green circles: $[Tc(CO)_3]^+$•Gluconate. Red triangles: $[Tc(CO)_3(H_2O)_2(OH)]$. Orange squares: TcO_4^-.

4.1.2.3 [Tc(CO)3]+ Complexes with NTA, EDTA, and DTPA

Tested polyaminocarboxylic chelators including NTA, EDTA and DTPA were observed to exhibit only weak affinity towards $[Tc(CO)_3]^+$ and low oxidative stability. The results are summarized in Tables 8 – 10 and Figures 7 – 9. In 5 M $NaNO_3$ / 0.1 M NaOH, the maximum fraction of the $[Tc(CO)_3]^+$•Ligand species accounted for 35%, 37% and 32% of the total Tc for NTA, EDTA and DTPA, respectively, taking an average of 4 days to reach maximum complexation. The corresponding fractions in the simulant solution were significantly lower and did not exceed 20 – 25%. The $[Tc(CO)_3]^+$ polyaminocarboxylate complexes exhibited poor stability and completely oxidized to TcO_4^- in 38, 30 and 25 days in 5 M $NaNO_3$ / 0.1 M NaOH solution as observed for NTA, EDTA, and DTPA, respectively. The corresponding decomposition times in the simulant were 20, 20 and 15 days.

Table 8. Formation Kinetics and Oxidative Stability of the $[Tc(CO)_3]^+$•NTA Complex in 5 M $NaNO_3$ / 0.1 M NaOH and Simulant Solutions Monitored by ^{99}Tc NMR Spectroscopy. Relative quantities of $[Tc(CO)_3(H_2O)_2(OH)]$, $[Tc(CO)_3]^+$•NTA, and TcO_4^- were determined by the integration of the corresponding resonances at -1070, -918 and near 0 ppm, respectively.

Time Elapsed	**Percent Fraction**		
	$[Tc(CO)_3(H_2O)_2(OH)]$	**$[Tc(CO)_3]^+$•NTA**	**TcO_4^-**
5 M $NaNO_3$ / 0.1 M NaOH / 3.2 mM Tc			
Start Day	0.95	0.05	0.01
1 day	0.75	0.19	0.06
2 days	0.66	0.26	0.08
3 days	0.60	0.31	0.10
4 days	0.56	0.34	0.13
6 days	0.52	0.30	0.18
8 days	0.47	0.26	0.27
12 days	0.38	0.21	0.41
16 days	0.29	0.17	0.55
20 days	0.21	0.12	0.67
26 days	0.13	0.08	0.79
32 days	0.06	0.04	0.91
38 days	0.01	0.00	0.99
0.47 M OH in simulant / 2.6 mM Tc			
Start Day	1.00	0	0.00
1 day	0.87	0.12	0.01
2 days	0.83	0.16	0.01
3 days	0.81	0.18	0.01
4 days	0.75	0.21	0.04
5 days	0.69	0.21	0.10
7 days	0.56	0.16	0.28
11 days	0.37	0.11	0.52
15 days	0.18	0.04	0.78
18 days	0.04	0.01	0.96
20 days	0.01	0	0.99

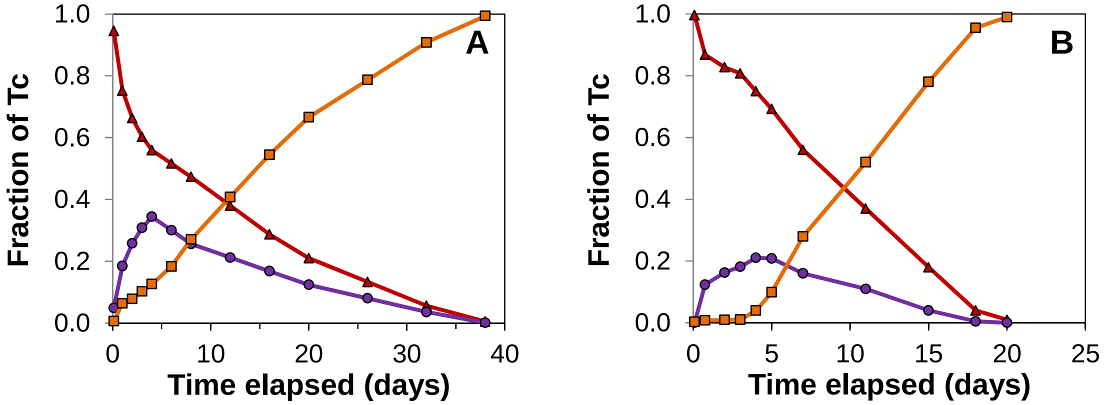

Figure 7. ^{99}Tc Time Speciation During Reaction of [$Tc(CO)_3(H_2O)_2(OH)$] with 0.1 M NTA in (A) 5 M $NaNO_3$ / 0.1 M NaOH and (B) Simulant. Purple circles: [$Tc(CO)_3$]$^+$•NTA. Red triangles: [$Tc(CO)_3(H_2O)_2(OH)$]. Orange squares: TcO_4^-.

Table 9. Formation Kinetics and Oxidative Stability of the [$Tc(CO)_3$]$^+$•EDTA Complex in 5 M $NaNO_3$ / 0.1 M NaOH and Simulant Solutions Monitored by ^{99}Tc NMR Spectroscopy. Relative quantities of [$Tc(CO)_3(H_2O)_2(OH)$], [$Tc(CO)_3$]$^+$•EDTA, and TcO_4^- were determined by the integration of the corresponding resonances at -1070, -916 and near 0 ppm, respectively.

Time Elapsed	**Percent Fraction**		
	[$Tc(CO)_3(H_2O)_2(OH)$]	**[$Tc(CO)_3$]$^+$•EDTA**	**TcO_4^-**
5 M $NaNO_3$ / 0.1 M NaOH / 3.2 mM Tc			
1 day	0.63	0.36	0.01
2 days	0.61	0.37	0.02
4 days	0.60	0.36	0.05
7 days	0.56	0.32	0.12
9 days	0.51	0.29	0.19
15 days	0.39	0.25	0.36
19 days	0.25	0.19	0.56
21 days	0.18	0.12	0.70
25 days	0.08	0.02	0.90
30 days	0.01	0.00	0.99
0.47 M OH in simulant / 2.6 mM Tc			
1 day	0.85	0.14	0.01
2 days	0.73	0.25	0.02
5 days	0.62	0.19	0.19
8 days	0.51	0.13	0.36
10 days	0.39	0.05	0.56
13 days	0.20	0	0.80
17 days	0.06	0	0.94
20 days	0.01	0	0.99

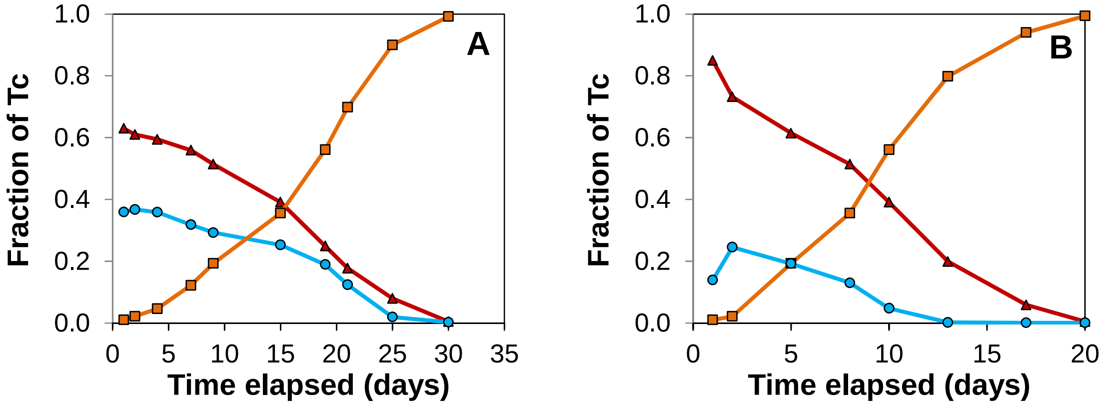

Figure 8. ^{99}Tc Speciation Over Time During Reaction of $[Tc(CO)_3(H_2O)_2(OH)]$ with 0.1 M EDTA in (A) 5 M $NaNO_3$ / 0.1 M NaOH and (B) Simulant. Light blue circles: $[Tc(CO)_3]^+$•EDTA. Red triangles: $[Tc(CO)_3(H_2O)_2(OH)]$. Orange squares: TcO_4^-.

Table 10. Formation Kinetics and Oxidative Stability of the $[Tc(CO)_3]^+$•DTPA Complex in 5 M $NaNO_3$ / 0.1 M NaOH and Simulant Solutions Monitored by ^{99}Tc NMR Spectroscopy. Relative quantities of $[Tc(CO)_3(H_2O)_2(OH)]$, $[Tc(CO)_3]^+$•DTPA, and TcO_4^- were determined by the integration of the corresponding resonances at -1070, -916 and near 0 ppm, respectively.

Time Elapsed	**Percent Fraction**		
(days)	**$[Tc(CO)_3(H_2O)_2(OH)]$**	**$[Tc(CO)_3]^+$•DTPA**	**TcO_4^-**
5 M $NaNO_3$ / 0.1 M NaOH / 3.2 mM Tc			
1	0.88	0.12	0.00
2	0.75	0.25	0.01
5	0.61	0.17	0.21
9	0.44	0.13	0.43
15	0.37	0.10	0.53
20	0.22	0.03	0.75
25	0.00	0.00	1
0.47 M OH in simulant / 2.6 mM Tc			
1	0.85		
2	0.73	0.14	0.01
5	0.61	0.25	0.02
8	0.43	0.19	0.19
10	0.35	0.13	0.36
15	0.20	0.09	0.56
20	0.00	0.02	0.78

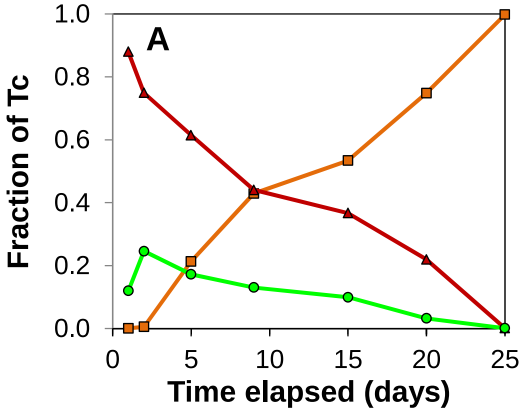

Figure 9. ^{99}Tc Time Speciation During Reaction of 3.2 mM [Tc(CO)$_3$(H$_2$O)$_2$(OH)] with 0.1 M DTPA in (A) 5 M NaNO$_3$ / 0.1 M NaOH and (B) Simulant. Light green circles: [Tc(CO)$_3$]$^+$•DTPA. Red triangles: [Tc(CO)$_3$(H$_2$O)$_2$(OH)]. Orange squares: TcO$_4^-$.

It was found that the decrease of the [Tc(CO)$_3$]$^+$•NTA, [Tc(CO)$_3$]$^+$•EDTA, or [Tc(CO)$_3$]$^+$•DTPA fractions was nearly linear with time as evident from the corresponding plots and the linear regression analysis (Figure 10).

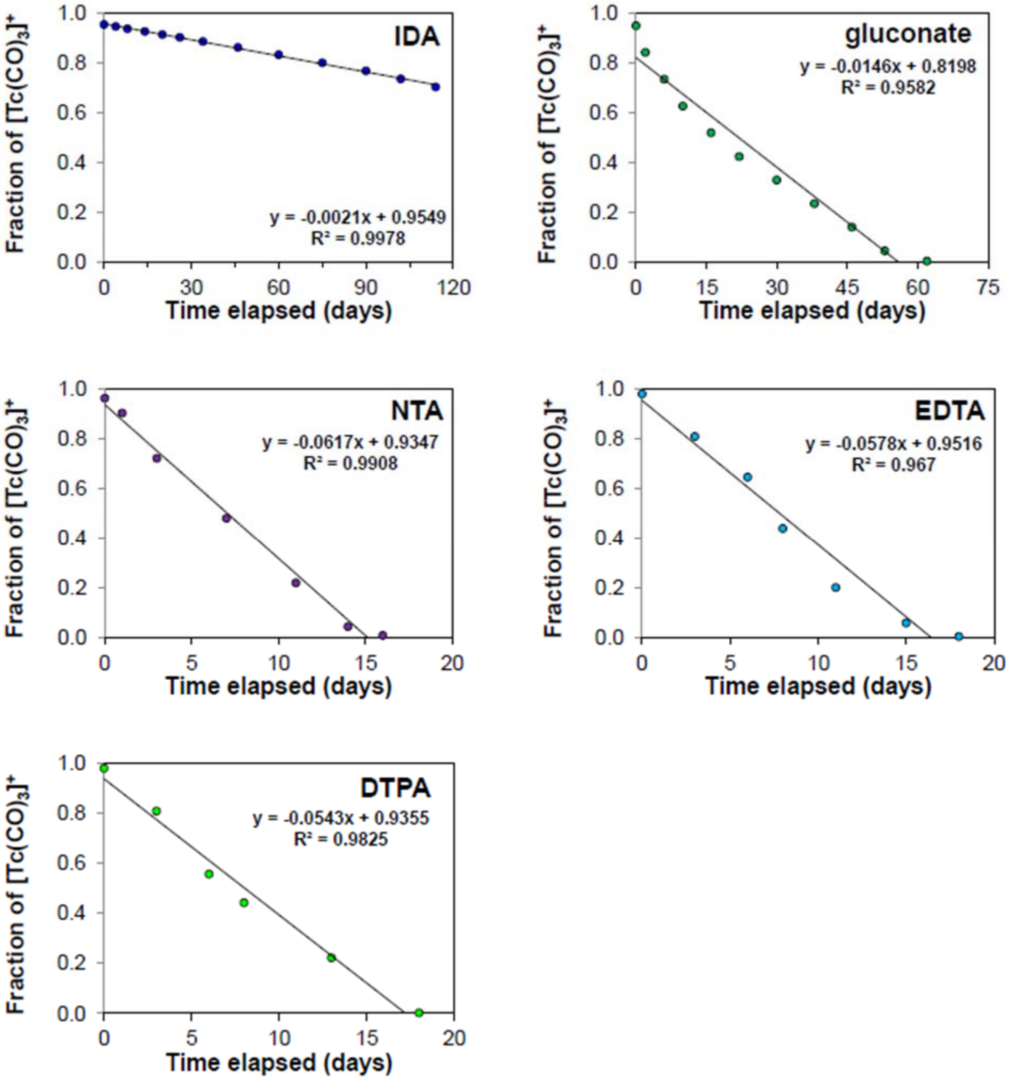

Figure 10. Kinetics of Decomposition of the $[Tc(CO)_3]^+$•Ligand Complexes in Simulant Solutions with Time

4.2 UV-vis Spectroscopy of $[Tc(CO)_3]^+$•Ligand

To gain better understanding of the $[Tc(CO)_3]^+$•Ligand complex formation, the kinetics of the $[Tc(CO)_3(H_2O)_2(OH)]$ conversion to $[Tc(CO)_3]^+$•Gluconate or $[Tc(CO)_3]^+$•IDA complexes was monitored by UV-vis spectroscopy. The test samples were prepared by the dissolution of solid $[Tc(CO)_3Cl_3]^{2-}$ precursor in 1 M NaOH solution in the absence of nitrate, which absorbs light in the UV-vis spectral region and interferes with Tc(I) measurements. The initial conversion of the $[Tc(CO)_3Cl_3]^{2-}$ precursor to $[Tc(CO)_3(H_2O)_2(OH)]$ species was confirmed by UV-vis spectroscopy. This solution was added to a solution of 0.2 M gluconate or 0.2 M IDA in 1 M NaOH matrix in 1:1 ratio, and the UV-vis spectra were acquired periodically.

The monitoring of the $[Tc(CO)_3]^+$•Gluconate complex formation is shown in Figure 11. The initial spectrum, collected ~ 5 minutes after solution preparation, exhibited a band at ~ 285 nm. The position and molar absorptivity of this band are nearly identical to those observed for the starting species, $[Tc(CO)_3 (H_2O)_2(OH)]$, in 1 M NaOH solution containing no gluconate (Levitskaia et al. 2014). With time, a new band at 264 nm appeared and increased in intensity. This band is assigned to the $[Tc(CO)_3]^+$•Gluconate complex. The intensity of this band reached maximum at about 4 hours post-solution preparation and exhibited significantly greater molar absorptivity than the UV band corresponding to the aqua $[Tc(CO)_3(H_2O)_{3-n}(OH)_n]^{1-n}$ species.

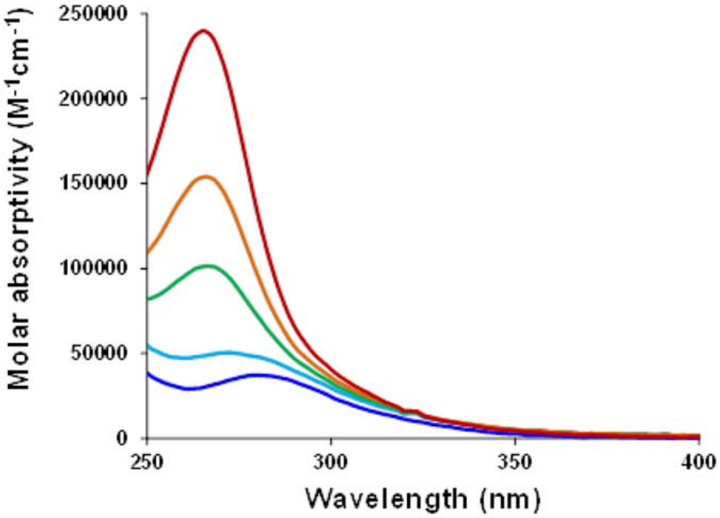

Figure 11. Time Dependent UV-vis Spectra of Aqueous $[Tc(CO)_3]^+$•Gluconate Complex: Spectra Collected at Different Time Intervals After Mixing Gluconate and $[Tc(CO)_3(H_2O)_2(OH)]$ Solutions. (dark blue trace) t= 5 minutes after addition, (light blue trace) t = 1 hour after addition, (green trace) t = 2 hours after addition, (orange trace) t = 3 hours after addition, (red trace) t = 4 hours after addition.

The monitoring results for the $[Tc(CO)_3]^+$•IDA complex are shown in Figure 12. Similar to the gluconate solution, the initial IDA UV-vis spectrum, collected ~5 minutes after solution preparation, exhibited a band at ~ 284 nm due to the starting $[Tc(CO)_3(H_2O)_2(OH)]$ compound. With time, a new band at ~289 with a shoulder at ~ 296 nm was observed to grow in. This band is assigned to the $[Tc(CO)_3]^+$•IDA complex. The intensity of this band reached a maximum within 15 minutes after solution preparation and exhibited nearly constant intensity thereafter. The 289 nm band exhibited significantly greater molar absorptivity than the UV bands corresponding to the other aqueous species of the form $[Tc(CO)_3(H_2O)_{3-n}(OH)_n]^{1-n}$.

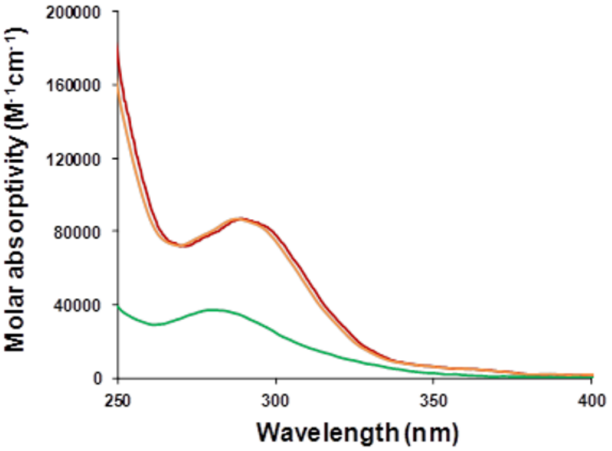

Figure 12. Time Dependent UV-vis Spectra of Aqueous $[Tc(CO)_3]^+$•IDA Complex: Spectra Collected at Different Time Intervals After Adding IDA to $[Tc(CO)_3(H_2O)_2(OH)]$: (green trace) t= 5 minutes after addition, (orange trace) t = 30 minutes after addition, (red trace) t = 2 hours after addition.

4.3 Stability of the Parr Reaction Products

4.3.1 Tc in Reacted Pseudo-Hanford Tank Supernatant Simulant Containing Gluconate and Noble Metals

4.3.1.1 Speciation Analysis

The product from the Parr reaction containing noble metals and gluconate showed the formation of a molasses-like brown precipitate within a brown supernatant. ^{99}Tc NMR spectroscopy of the supernatant revealed that > 90% TcO_4^- was reduced. The NMR spectrum of the liquid fraction exhibited three Tc(I) resonances at -1094, -1232, and -1254 ppm corresponding to the Tc(I)-tricarbonyl gluconate species. The exact structure of these species has not been elucidated. The chemical shift of the $[Tc(CO)_3]^+$•Gluconate resonances observed for the reacted simulant are nearly identical to those generated by the dissolution of $[Tc(CO)_3(H_2O)_2(OH)]$ in either 5 M $NaNO_3$ / 0.1 M NaOH / 0.1 M sodium gluconate solution or in 0.1 M sodium gluconate dissolved in the simulant (Sections 4.1.1.2 and 4.1.2.2), with the resonance at -1100 ppm being slightly shifted to -1094 ppm. One difference between these spectra is the narrower line widths associated with resonances found in the CO/H_2-reacted simulant. This feature, along with the inability to simultaneously adjust the phases of all of the resonances in the sample, is attributed to the presence of paramagnetic constituents, such as Tc(IV) and Tc(VI). This is consistent with the observation that intensity of the TcO_4^- resonance measured before the start of the reaction (TcO_4^- being the only Tc species present in the sample before the reaction and therefore accounting for total Tc in the sample) was greater than the sum of the intensities of the TcO_4^- resonance appearing in the vicinity of 0 ppm and the $[Tc(CO)_3]^+$ resonances at -1094, -1232 and -1254 ppm post reaction completion. This indicates that in this reaction, TcO_4^- is reduced to NMR silent paramagnetic species, such as Tc(II, IV, and/or VI), in addition to Tc(I).

When summed, Tc(I) and Tc(VII) together could not account for the total Tc present in the sample (Table 11). It should be noted that partitioning of the Tc(I) and Tc(VII) species to the solid fraction of the reaction product is unlikely due their high aqueous solubility. This implies that a significant portion of Tc in the sample exists as paramagnetic non-pertechnetate Tc(II, IV, and/or VI) species in the liquid and/or solid fractions of the reacted simulant. This contributes to a significant fraction of Tc present in the sample as shown in the last column of Table 11.

Table 11. Time Monitoring of the Observed ^{99}Tc NMR Resonances in the Liquid Fraction of the CO/H_2-reacted Pseudo-Hanford Tank Supernatant Simulant (composition of the simulant is given in Table 1) Containing 0.1 M Gluconate and Catalytic Noble Metals. Each resonance area was determined by the integration and normalized for the number of scans. The integrals of the resonances corresponding to the $[Tc(CO)_3]^+$•Gluconate complex are shown as a sum of integrals of the individual -1094, -1232, and -1254 ppm resonances.

Time Elapsed	**NMR Active Species in the Liquid Fraction**			**Sum of Liquid and Solid Fractions**
(days)	**$[Tc(CO)_3]^+$ (%)**	**TcO_4^-(%)**	**Tc (I) + Tc (VII) (%)**	**NMR inactive non-TcO_4^- (%)**
Before reaction	N/A	100% [a]	N/A	N/A
0.04	63%	6%	69%	31%
0.17	55%	6%	61%	39%
0.79	49%	6%	55%	45%
3	45%	6%	50%	50%
5	39%	9%	48%	52%
8	38%	9%	47%	53%
19	34%	14%	48%	52%
49	31%	22%	54%	46%
99	32%	28%	60%	40%
150	32%	35%	67%	33%
224	29%	45%	74%	26%
298	26%	54%	80%	20%
365	23%	62%	85%	15%

[a] Corresponds to the total Tc in the sample, which was added to the simulant as TcO_4^-.

To probe the presence of the paramagnetic constituents Tc(II, IV, and/or VI) in the sample, both solid and liquid fractions of the reacted simulant were analyzed by EPR spectroscopy (Figure 13 and Figure 14). The spectrum of the precipitate exhibits at least three distinct signals as shown in Figure 13. The low-field end of the spectrum is complicated with two overlapping signals. A large single signal around 1,600 Gauss dominates this portion of the spectrum and has a g-value that is commonly associated with Fe clusters. Iron clusters are commonly observed in EPR spectra due to external contamination on the instrumentation, specifically the sample holder. However, there is a signal spanning either side of the low-field singlet, split into what we approximate to be 10 lines. This would correspond to hyperfine splitting due to the ^{99}Tc nucleus with a nuclear spin of 9/2. The shift in hyperfine signal of this peak is surprising to us and may be explained as a half-field transition in which the electron spin density associated with the ^{99}Tc nucleus is strongly coupled to another metal center with a total electron spin of 1/2.

The high-field portion of the spectrum shows a single spectral signature at approximately 3100 Gauss, it displays what appears to be a signal from a ^{99}Tc nucleus in a relatively high symmetry chemical environment. Based on the narrow line width, g-value (analogous to chemical shift in NMR), and similar hyperfine splitting constants observed in this spectrum as those observed for electrochemically generated Tc (VI) species, which yielded an excellent least-squares simulation of the data with $S = ½$, (Levitskaia et al. 2015) we believe this signal is due to a chemically synthesized Tc(VI) species. It is important to note that under the conditions previously used to electrochemically generate Tc (VI) species for EPR spectroscopy, the oxidation state could be inferred by comparing the number of electrons used to reduce Tc(VII) to moles of Tc(VII) present. In this study, reaction conditions do not allow for monitoring of the chemical reductant, H_2, to Tc (VII) ratio, and for this reason other oxidation states could be potentially responsible for the signal, one option being Tc(II) which from the standpoint of d-orbital electron configuration replaces the unpaired electron in Tc(VI) species with a hole in Tc (II) species yielding analogous electronic microstates, and subsequently similar EPR spectra.

We consider other oxidation states such as Tc(IV) to be considerably less likely. The main driving force for this conclusion is the narrow line widths, which strongly suggest a system with an electronic spin of ½. EXAFS data (Lukens et al. 2002) suggests that Tc(IV) under similar conditions should have a coordination number of six. Due to the large d-orbital splitting commonly associated with second and third row transition metals, Tc in such a pseudo octahedral field should provide a system in which the electron spin is greater than ½ (Lukens et al. 2002). Such $S > ½$ systems result in broad hyperfine signals due to interaction between the electron spins.

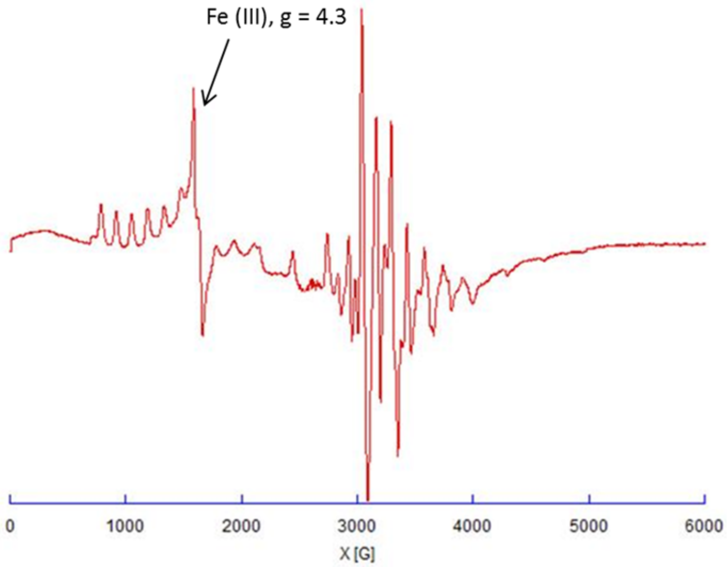

Figure 13. ^{99}Tc EPR Spectrum of the Solid Fraction of the CO/H_2-reacted Pseudo-Hanford Tank Supernatant Simulant (composition of the simulant is given in Table 1) Containing 0.1 M Gluconate and Catalytic Noble Metals

The liquid fraction of the reacted simulant produced a similar EPR spectrum (Figure 14), which is explained in an analogous manner to the spectrum produced by the precipitate. The most prominent difference between the two spectra is the relative ratio of the low-field ^{99}Tc signal to the other two signals present in the spectra. There is a dramatic reduction of the low-field signal intensity relative to both the high-field ^{99}Tc signal and the large singlet present at approximately 1,600 Gauss in the liquid fraction compared to the solid EPR spectrum. This is supportive that the singlet is an environmental contaminant (likely Fe) rather than a species chemically associated with ^{99}Tc.

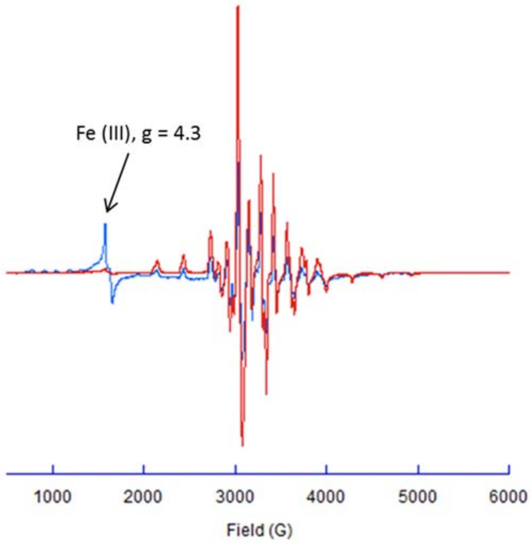

Figure 14. ^{99}Tc EPR Spectra of the Liquid Fraction of the CO/H_2-reacted Pseudo-Hanford Tank Supernatant Simulant (composition of the simulant is given in Table 1) Containing 0.1 M Gluconate and Catalytic Noble Metals Collected 5 Days After Generation of the Sample (blue trace) and Approximately 365 Days Later (red trace)

4.3.1.2 Time Monitoring

Time monitoring of the speciation of the ^{99}TcNMR-active compounds in the liquid fraction of the reacted simulant revealed intriguing trends (Table 11, Figure 15). Pertechnetate increase is gradual and nearly linearly with time starting at day 5 through 1 year post sample preparation. On the other hand, the relative concentration of $[Tc(CO)_3]^+$ steeply decreased during the first 19 days, then remained nearly constant during the following 7 months, and started gradually decreasing after that. This suggests that the $[Tc(CO)_3]^+$•Gluconate species oxidized to NMR-inactive paramagnetic species such as Tc(II, IV, and/or VI) and not to TcO_4^-. In turn, the increase of the TcO_4^- fraction must be due to the oxidation of Tc(II, IV, and/or VI) taking into account that it occurred during the time when $[Tc(CO)_3]^+$•Gluconate concentration remained nearly unchanged.

The $[Tc(CO)_3]^+$ species generated by the chemical reduction of TcO_4^- under high temperature and pressure in the presence of gluconate and noble metals, demonstrated a unprecedented oxidative stability (Table 11, Figure 15) of non-pertechnetate species over the period of one year. ^{99}Tc NMR monitoring demonstrates that about 37% of the $[Tc(CO)_3]^+$•Gluconate species initially generated in the liquid fraction of the reacted simulant remain in the sample after storing in air and exposed to light for a year. This is significantly longer life time than observed for the $[Tc(CO)_3]^+$•Gluconate species generated by addition of $[Tc(CO)_3(H_2O)_2(OH)]$ to the simulant containing gluconate or gluconate and noble metals, which completely decomposed in 64 and 78 days, respectively (Table 5 and Table 7). The oxidation kinetics of the $[Tc(CO)_3]^+$•Gluconate species in the reacted simulant exhibited a complicated profile with 3 distinct time-dependent regions (Figure 15) including initial steep reduction in concentration for a short period of time (5 days) followed by long time of very slow rate of oxidation (about 220 days), which very gradually increased after day 224. The monitoring of this sample is currently continuing.

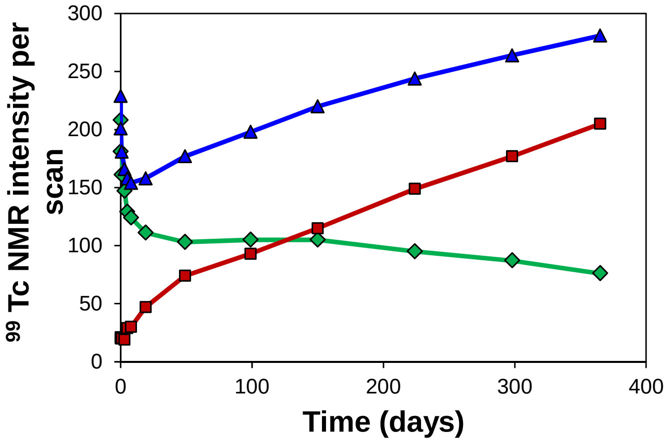

Figure 15. Time Monitoring of $[Tc(CO)_3]^+$ and TcO_4^- Species in the Solution Fraction of the CO/H_2-reacted Pseudo Hanford Tank Supernatant Simulant (composition of the simulant is given in Table 1) Containing 0.1 M Gluconate and Catalytic Noble Metals. Red squares: TcO_4^-. Green diamonds: combined $[Tc(CO)_3]^+$ species corresponding to the resonances at -1094, -1232 and -1254 ppm. Blue triangles: total NMR-active ^{99}Tc species.

The EPR measurements of the liquid fraction of the reacted simulant contacted shortly after generation of the sample and one year later have very similar high-field spectra (Figure 14) revealing that paramagnetic Tc(II and/or VI) are surprisingly stable and remain in the sample for a long time. This suggests that low oxidation state Tc(II and/or VI) species may significantly contribute to the non-pertechnetate Tc occurring in the tank waste.

4.3.2 Pseudo-Hanford Tank Supernatant Simulant Containing Gluconate Without Noble Metals

4.3.2.1 Speciation Analysis

To evaluate the role of gluconate in the reduction of TcO_4^- in tank supernate simulant, the reduction reaction was performed using simulant containing 0.1 M gluconate without noble metals keeping other conditions the same. Upon completion of the reaction, the reaction mixture contained only liquid of pink color, no solid (precipitate) was generated. ^{99}Tc NMR characterization of the resulting solution exhibited a single weak resonance at near 0 ppm corresponding to unreacted TcO_4^- no formation of $[Tc(CO)_3]^+$, Tc(V), or other NMR-active Tc species was observed (data not shown). Based on the comparison of the ^{99}Tc NMR spectra acquired using simulant prior- and post-reaction, it was determined that about 70 – 75% TcO_4^- was reduced to the paramagnetic Tc(II, IV, and/or VI) species in the intermediate oxidation states, and that the reduction did not proceed to formation of Tc(I) species.

The reacted simulant was subjected to the EPR spectroscopic analysis (Figure 16). The spectrum displays a 10-line pattern at ~3100 G, and appears to be a signal from a ^{99}Tc nucleus in a relatively high symmetry chemical environment. The EPR spectra strongly resembles that observed in the high field from the reduction product obtained in presence of gluconate and noble metals (Figure 17; see Figure 17 for an overlay of the two spectra), and is attributed to Tc(VI) or Tc(II) species consistent with the NMR analysis. EPR spectroscopy experiments showed no presence of Tc(IV) species.

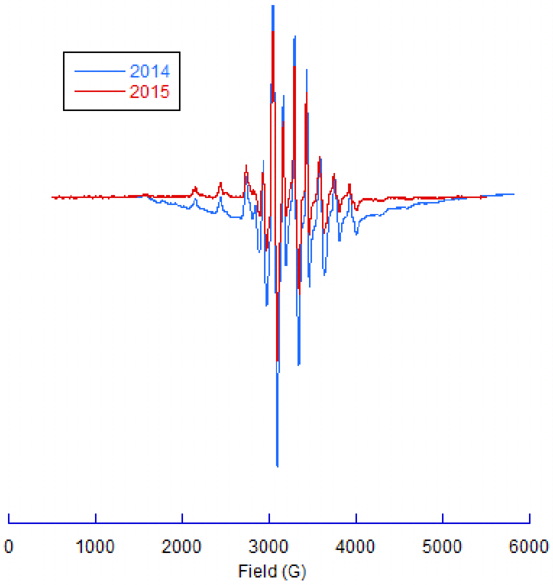

Figure 16. ^{99}Tc EPR Spectra of the Liquid Fraction of the CO/H_2-reacted Pseudo-Hanford Tank Supernatant Simulant (composition of the simulant is given in Table 1) Containing 0.1 M Gluconate Collected and 5 Days After Generation of the Sample (blue trace) and Approximately 365 Days Later (red trace)

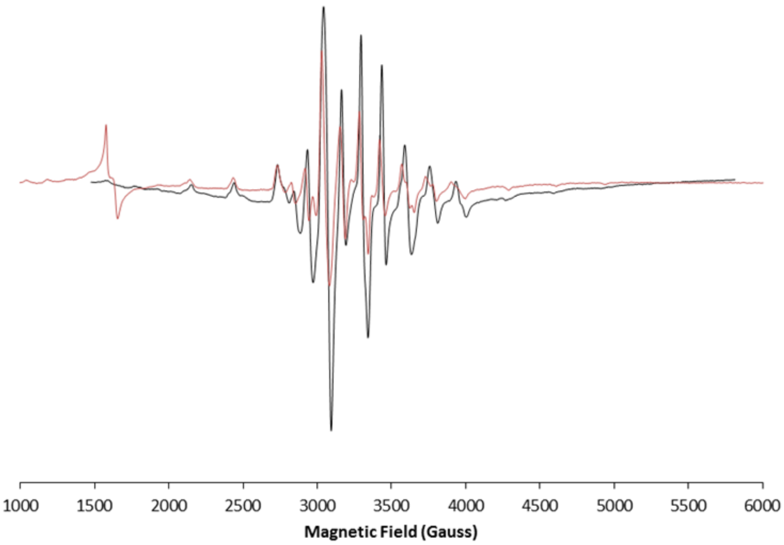

Figure 17. Overlay of EPR Signal From Chemically Reduced Tc Species in the Presence of Both Gluconate and Noble Metals (red trace) and in the Presence of Gluconate But Absence of Noble Metals (black trace) at Day 5 After Generation of the Samples

4.3.2.2 Time Monitoring

The most remarkable aspect of the reacted simulant containing gluconate without noble metals is the persistence of the Tc(II and/or VI) non-pertechnetate species. The sample, generated in 2014, preserved under ambient laboratory conditions for a period of 12 months displayed an EPR strong signal with identical profile of the original (5-day) spectrum and only slightly reduced intensity suggesting that the chemical integrity of the reduced Tc species is preserved (Figure 16).

Concentration of TcO_4^- in the reacted simulant slowly increased with time (Table 12). The Tc(VII) ingrowth observed one year post sample generation corresponds to the oxidation of only about 20% of the non-pertechnetate Tc(II and/or VI) species generated by the chemical reduction. This finding strongly suggests that the stable non-pertechnetate species in the intermediate oxidation states can exist in the tank waste supernatants. We however do acknowledge that the radiation fields present in real tank waste samples may influence the stability of non-pertechnetate species. This warrants the evaluation of the stability of non-pertechnetate species in presence of radiation fields.

Table 12. ^{99}Tc NMR Time Monitoring of the CO/H_2-reacted Pseudo-Hanford Tank Supernatant Simulant (composition of the simulant is given in Table 1) Containing 0.1 M Gluconate. The reported data correspond to the liquid fraction of reaction mixture as sample contained no solids.

Time Elapsed (days)	TcO_4^- (%)	Percent NMR Inactive Non-TcO_4^- (%)
Before reaction	100%[a]	N/A
0.05	25%	75%
0.3	24%	76%
1	26%	74%
3	27%	73%
6	27%	73%
10	27%	73%
21	27%	73%
72	30%	70%
130	32%	68%
200	35%	65%
381	38%	62%

[a] Corresponds to the total Tc in the sample, which was added to the simulant as TcO_4^-.

4.3.3 Pseudo-Hanford Tank Supernatant Simulant Containing Noble Metals Without Gluconate

4.3.3.1 Speciation Analysis

To evaluate the role of noble metals in the reduction of TcO_4^- in simulant, the reduction reaction was performed using simulant containing noble metals without gluconate keeping other conditions the same including reducing atmosphere, temperature and the duration of the reaction. Upon completion of the reaction, the reacted simulant contained greenish-brown precipitate and a liquid fraction of brown color. Based on the ^{99}Tc NMR analysis of the simulant prior to reaction and of the liquid fraction of the reacted simulant, it was determined that about 85 – 90% TcO_4^- was reduced (Table 13).

Table 13. ^{99}Tc NMR Time Monitoring of the Liquid Fraction of the CO/H_2-reacted Pseudo-Hanford Tank Supernatant Simulant (composition of the simulant is given in Table 1) Containing Noble Metals. The area of each resonance was determined by the integration of the energy peaks previously identified and normalized for the number of scans.

Time Elapsed	**NMR Active Species in the Liquid Fraction**			**Sum of Liquid and Solid Fractions**
(days)	**$[Tc(CO)_3]^+$ (%)**	**TcO_4^-(%)**	**Tc (I) + Tc (VII) (%)**	**NMR inactive non-TcO_4^- (%)**
Before reaction	N/A	100%[a]	N/A	N/A
0.05	72%	12%	84%	16%
3	44%	10%	54%	46%
5	38%	15%	53%	47%
8	36%	16%	52%	48%
19	31%	24%	55%	45%
60	18%	51%	68%	32%
125	11%	68%	79%	21%
170	0%	83%	83%	17%
330	0%	91%	91%	9%

[a] Corresponds to the total Tc in the sample, which was added to the simulant as TcO_4^-.

The ^{99}Tc NMR spectrum of the solution fraction taken ~1 hour after the reaction showed a single new resonance at -1092 ppm. While the position of this resonance is similar to one of the resonances observed when the reaction was performed in the presence of gluconate, it is significantly more narrow and the positional overlap is considered to be coincidental. The position of the -1092 ppm resonance is shifted downfield with respect to $[Tc(CO)_3(H_2O)_2(OH)]$ resonance appearing at about -1070 ppm. So it was concluded that the -1092 ppm resonance corresponds to the Tc(I) $[Tc(CO)_3]^+$ species, while the elucidation of the exact structure of these species requires additional experimentation.

When summed, Tc(I) and Tc(VII) together could not account for the total Tc present in the sample (Table 13; right hand column). This implies that a significant portion of Tc in the sample exists as paramagnetic non-pertechnetate Tc(II, IV, and/or VI) species in the liquid and/or solid fractions of the reacted simulant. Similar results were obtained for the reacted simulant containing both gluconate and noble metals (Section 4.1.1.2).

4.3.3.2 Time Monitoring

Time monitoring of the speciation of the Tc NMR-active compounds in the liquid fraction of the reacted simulant revealed interesting trends (Table 13, Figure 18, and Figure 19). Pertechnetate fraction decreased during first 3 – 5 days post reaction termination suggesting that the Tc(VII) reduction continued even when removed from the CO/H_2 atmosphere. This initial decrease was followed by a steady nearly liner increase of the TcO_4^- concentration with time. The $[Tc(CO)_3]^+$ fraction steeply decreased during the first 19 days, followed by the gradual decrease and complete decomposition at about day 170 post sample generation. Taken together, the kinetic profiles of the TcO_4^- and $[Tc(CO)_3]^+$ species suggest that paramagnetic species such as Tc(II, IV, and/or VI) play an important role in the redox behavior of Tc.

After day 170, the concentration of TcO_4^- approached the total Tc present in the sample suggesting complete oxidation of all non-pertechnetate species.

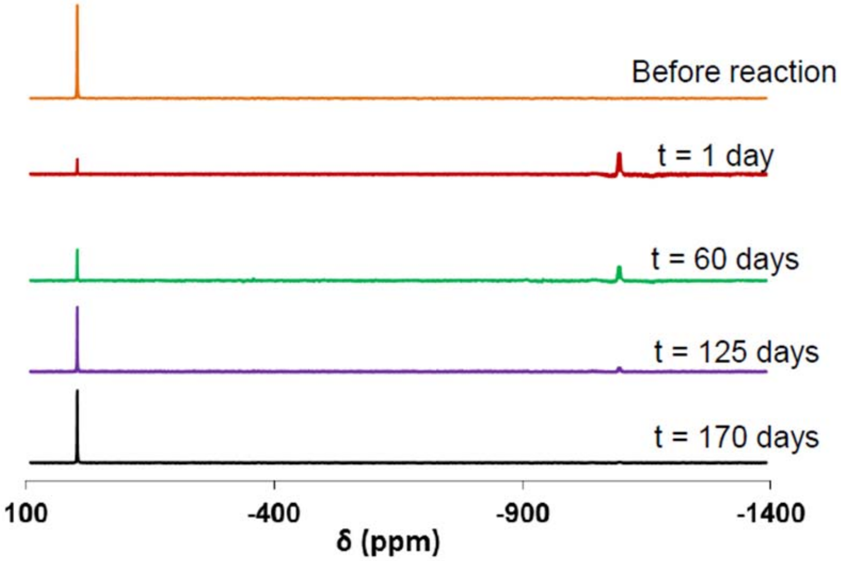

Figure 18. ^{99}Tc NMR Time Monitoring of the Liquid Fraction of the CO/H_2-reacted Pseudo-Hanford Tank Supernatant Simulant (composition of the simulant is given in Table 1) Containing Noble Metals

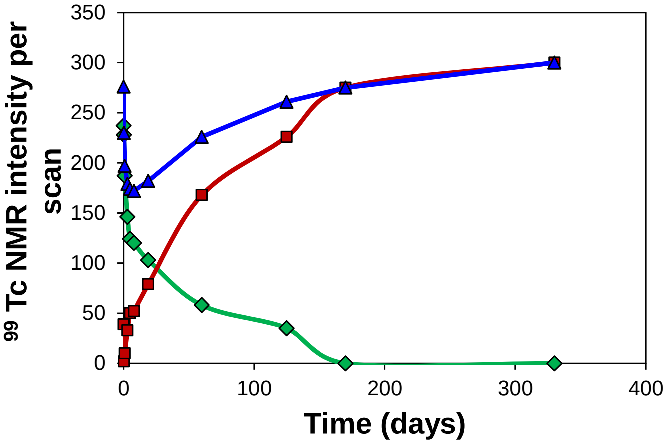

Figure 19. Time Monitoring of $[Tc(CO)_3]^+$ and TcO_4^- Species in the Solution Fraction of the CO/H_2-reacted Pseudo Hanford Tank Supernatant Simulant (composition of the simulant is given in Table 1) Containing Catalytic Noble Metals. Red squares: TcO_4^-. Green diamonds: $[Tc(CO)_3]^+$ species corresponding to the resonance at -1094 ppm. Blue triangles: total NMR-active ^{99}Tc species.

4.3.4 Pseudo-Hanford Tank Supernatant Simulant Without Noble Metals and Without Gluconate

4.3.4.1 Speciation Analysis

The control Tc(VII) reduction reaction was performed using simulant without noble metals and without gluconate keeping other conditions the same including reducing atmosphere, temperature and the duration of the reaction.

Upon completion of the reaction, the reacted simulant contained greenish-brown precipitate and supernatant of brown color. Based on the ^{99}Tc NMR analysis of the simulant prior to reaction and of the liquid fraction of the reacted simulant, it was determined that about 10% TcO_4^- was reduced (Table 14). A small amount of $[Tc(CO)_3]^+$ species was generated during the reaction. The position of the NMR resonance at -1075 ppm was attributed to the $[Tc(CO)_3(H_2O)_2(OH)]$ product. At each time point, the sum of the Tc(VII) and Tc(I) concentrations is significantly smaller than the total Tc content in the sample suggesting the presence of the paramagnetic Tc(II, IV, and/or VI) species. After, 50 days, while the total amount of $[Tc(CO)_3]^+$ species had completely decomposed in the liquid fraction, only about ½ of the total TcO_4^- had been regenerated from the starting materials.

Table 14. ^{99}Tc NMR Time Monitoring of the Liquid Fraction of the CO/H_2-reacted Pseudo-Hanford Tank Supernatant Simulant (composition of the simulant is given in Table 1). The area of each resonance was determined by the integration of previously identified peaks and normalized for the number of scans.

Time Elapsed	**NMR Active Liquid Fraction**			**Sum of Liquid and Solid Fractions**
(days)	**$[Tc(CO)_3]^+$ (%)**	**TcO_4^- (%)**	**Tc (I) + Tc (VII) (%)**	**NMR inactive non-TcO_4^- (%)**
Before reaction	N/A	100%[a]	N/A	N/A
0.04	11%	7%	18%	82%
1	10%	8%	18%	82%
2	9%	8%	18%	82%
6	8%	10%	18%	82%
10	8%	11%	19%	81%
15	7%	13%	20%	80%
23	5%	15%	20%	80%
29	4%	17%	21%	79%
37	1%	22%	23%	77%
45	1%	22%	23%	77%
49	0%	23%	23%	77%
70	0%	26%	26%	74%
110	0%	30%	30%	70%
200	0%	45%	45%	55%

[a] Corresponds to the total Tc in the sample, which was added to the simulant as TcO_4^-.

4.3.4.2 Time Monitoring

Time monitoring of the speciation of the Tc NMR-active compounds in the liquid fraction of the reacted simulant revealed nearly linear profiles of the decomposition of the $[Tc(CO)_3(H_2O)_2(OH)]$ species and formation of re-generated TcO_4^- (Figure 20). The rate of $[Tc(CO)_3(H_2O)_2(OH)]$ oxidation was found to be nearly identical to that observed for these species in the unreacted simulant (Section 4.1.1.2, Table 4). At about day 49 after sample generation, all $[Tc(CO)_3(H_2O)_2(OH)]$ and part of Tc(II, IV, and/or VI) oxidized to TcO_4^- (Table 14).

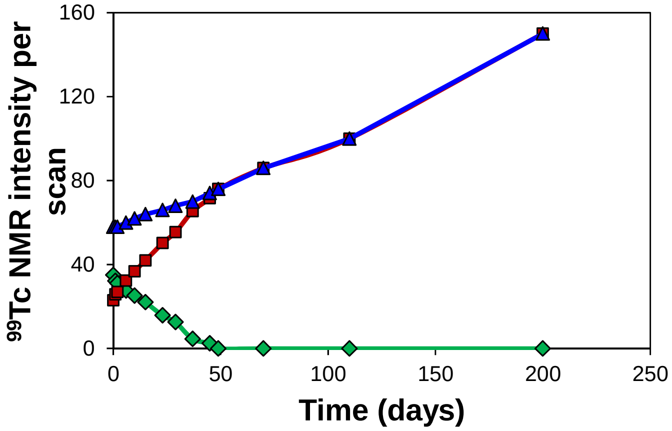

Figure 20. Time Monitoring of $[Tc(CO)_3]^+$ and TcO_4^- Species in the Solution Fraction of the CO/H_2-reacted Pseudo-Hanford Tank Supernatant Simulant (composition of the simulant is given in Table 1). Red squares: TcO_4^-. Green diamonds: $[Tc(CO)_3]^+$ species corresponding to the resonance at -1094 ppm. Blue triangles: total NMR-active ^{99}Tc species.

4.3.5. Discussion: *in situ* Generated Non-pertechnetate Species

In August – September 2014, a series of samples was generated by reacting NH_4TcO_4 solution in pseudo-Hanford tank supernatant simulant with and without gluconate and/or catalytic noble metals with CO/H_2 in a Parr vessel under elevated pressure and temperature. The obtained products were analyzed in September 2014 shortly after reaction termination and monitored for one year. The comparison of the initial results and those obtained about one year later is given in Tables 15 and 16. Note remarkable stability of Tc(VI) and Tc(I) as $[Tc(CO)_3]^+$•Gluconate in the reacted simulant.

Table 15. Comparison of Tc Speciation in the CO/H_2-reacted Pseudo Hanford Tank Supernatant Simulants Shortly (within 1 week) After Sample Generation and One Year Later

Reaction Medium	**September 2014 Observations**	**September 2015 Observations**
Simulant + 0.1 M gluconate + catalytic noble metals	Visual observations Light-brown solution + dark brown precipitate ^{99}Tc NMR analysis Solution contains 6% of initial TcO_4^- 63% is reduced to Tc(I) as $[Tc(CO)_3]^+$•Gluconate Sample contains 11% Tc(II/VI) non-TcO_4^- and 20% insoluble Tc(IV) ^{99}Tc EPR analysis Single Tc(II/VI) species in solution Two different Tc(II/VI) species in precipitate	Visual observations Light-brown solution + reduction in the amount of dark brown precipitate ^{99}Tc NMR analysis Solution contains 62% of initial TcO_4^- **23% remains as $[Tc(CO)_3]^+$•Gluconate** **11% remains as Tc(II/VI) soluble non-TcO_4^-** ^{99}Tc EPR analysis **Single Tc(II/VI) species in solution**
Simulant + catalytic noble metals	Visual observations Brown solution + greenish-brown precipitate ^{99}Tc NMR analysis Solution contains 12% of initial TcO_4^- 72% is reduced to Tc(I) as derivative of $[Tc(CO)_3]^+$ Overall sample (solids and liquid) contains 16% Tc(II/IV/VI) non-TcO_4^-	Visual observations Brown solution + reduction in the amount of black precipitate ^{99}Tc NMR analysis 91% TcO_4^- is regenerated in solution 3% non-TcO_4^- remains in solution while 6% non-TcO_4^- remains as solid
Simulant + 0.1 M gluconate	Visual observations Pink solution, **no precipitate formed** ^{99}Tc NMR analysis Solution contains 25% of initial TcO_4^- no Tc(I) is found in solution Solution contains 75% Tc(II/VI) non-TcO_4^- ^{99}Tc EPR analysis Single Tc(II/VI) species in solution	Visual observations Pink solution, no precipitate ^{99}Tc NMR analysis Solution contains 37% of initial TcO_4^- **63% remains as Tc(II/VI) non-TcO_4^-** ^{99}Tc EPR analysis **Single Tc(II/VI) species in solution**
Simulant only	Visual observations Sand-color solution + dark brown/black precipitate ^{99}Tc NMR analysis Solution contains 7% of initial TcO_4^- 11% is reduced to Tc(I) as $[Tc(CO)_3(H_2O)_2(OH)]$ Liquid fraction contains ~18% Tc(II/IV/VI) non-TcO_4^- suggesting the rest in reduced to insoluble Tc(IV)	Visual observations Sand-color solution + reduction in dark brown/black precipitate ^{99}Tc NMR analysis All non-TcO_4^- in the liquid fraction decomposed 46% of initial TcO_4^- is regenerated in solution suggesting re-oxidation of non-TcO_4^- from solid to solution TcO_4^-

Table 16. Comparison of Relative Quantities of TcO_4^- and Non-Pertechnetate Tc in the CO/H_2-reacted Pseudo Hanford Tank Supernatant Simulants Shortly (within 1 week) After Sample Generation and One Year Later

Time	**Liquid Fraction a)**			**Solid Fraction (%) b)**
	TcO_4^- (%)	**non-TcO_4^- (%)**		
		Tc(I)	**Tc(II/VI)**	
Parr reaction/ gluconate/ noble metals				
Immediately after reaction	6	63	11	20
468 days after reaction	62	23	11	4
Parr reaction/ gluconate				
Immediately after reaction	25	0	75	N/A
450 days after reaction	38	0	62	
Parr reaction/ noble metals				
Immediately after reaction	12	72	3	13
440 days after reaction	91	0	3	6
Parr reaction without gluconate without noble metals				
Immediately after reaction	7	11	0	82
458 days after reaction	46	0	0	54

a) Determined by ^{99}Tc NMR
b) Determined by LSC

The observed results highlight the importance and relevance of non-pertechnetate species in the liquid fraction of tank waste in general, and Tc(II/VI) species in particular. While TcO_4^- is the most stable and abundant natural form of Tc in tank wastes, the data on Tc(II) are essentially non-existent and information on Tc(VI) species remains scarce (Rard 1983; Rard 2005). While in some cases, solids of Tc(VI) of formulae $[(CH_3)_4N]_2TcO_4$ have been isolated (Astheimer et al. 1975), such isolation has been reported to be possible only under moisture free conditions. Presence of moisture has been reported to catalyze the fast oxidation of TcO_4^{2-} to TcO_4^-. Tc(VI) halides of the form $TcCl_6$ have been reported in the presence of a concentrated stream of Cl_2 gas, but are prone to rapid disproportionation (Colton 1962). TcF_6 has also been reported to exist in solid, liquid and vapor states, but no reports exist on the compound in aqueous solutions (Rard et al. 2005; Osborne et al. 1977; Selig et al. 1962). Colton et al. (1968) reacted thionyl chloride (SO_2Cl_2, an extremely strong Lewis acid) with NH_4TcO_4 to prepare the thionyl chloride adduct $(NH_4)_2[TcO_2Cl_4]$ SO_2Cl_2, which contains Tc(VI), but this was observed to rapidly disintegrate to Tc(VII). More recently, several Tc(VI) complexes have been isolated and characterized structurally, including $TcOF_4$ and $(TcOF_4)_3$ (Rard et al. 1999). However, the solution chemistry of Tc(VI) remains elusive, mainly owing to the instability of Tc(VI). A one electron reduction is sometimes observed in basic media, but the Tc(VI) species produced is very unstable and rapidly disproportionates to TcO_4^- and a Tc(IV) species or TcO_4^- and a Tc(V) species (Rard et al. 1999). Majumdar et al. (1969) reported the formation of Tc(VI) by chemical reduction of TcO_4^- with hydrazine. Electrochemical reduction of TcO_4^- has also been used to generate Tc(VI) species of the form TcO_4^{2-} in aqueous solutions of various alkalinity (Kiesel and Feldberg, 1969). Similar Tc(VI) species have also been generated using pulsed electron beams. However, it was observed that the Tc(VI) species generated in these studies were extremely short-lived and underwent rapid disproportionation within minutes to Tc(VII) and Tc(V) (Rard 1999). It was found that in alkaline solutions TcO_4^{2-} had a lifetime of at least 10 msec, but that noticeable reactions occurred within 50 ms (Deutsch et al. 1978; Hurst 1980). Kissel and Feldberg studied the decomposition kinetics of TcO_4^{2-} in 0.001 to 0.10 M NaOH and found the disproportionation to be slower at higher NaOH concentrations (Kissel and Feldberg, 1969; Krychkov et al. 1979). It was only recently that we observed that at very high ionic strength matrices, the stability of the Tc(VI) species can be enhanced and more so in presence of chelators. This is consistent with the observations of Takayama et al. (1995) who reported the formation of an EDTA coordinated Tc(VI) dimer in solution. The high ionic strength matrices and the presence of chelators can extend the half-life of Tc(VI) product for years, as observed in our Parr reaction products. This observation is incredibly important as it can have significant implications in the chemical and redox speciation of Tc in tank waste supernatants.

Another unusual observation is the stability of the non-pertechnetate Tc in solid fractions. Based on EPR measurements of the solid reaction product isolated from the reacted simulant containing gluconate and noble metals as well as the established observations that the oxidative stability of Tc(IV) is very limited it is possible that the major non-pertechnetate solid fraction is Tc(II/VI). However, the dark brown color of the precipitates in our tests does not allow us to rule out formation of more common Tc(IV) precipitates. Additional experimentation is needed to elucidate the structure of these non-pertechnetate species both in solution and in precipitates.

5.0 Conclusions

In this work, considerable achievements were made toward verifying that the Tc(I)-tricarbonyl species is a viable candidate for the source of alkaline-soluble, non-pertechnetate Tc in the Hanford tank supernatants. This work confirmed that the Tc species based on the $[Tc(CO)_3]^+$ center can be produced by the laboratory synthetic route and that a potential route exists for their production in the alkaline Hanford tank wastes. These non-pertechnetate species are sufficiently stable under the conditions associated with Hanford tank supernatants. However, considerable work remains, specifically to achieve control over Tc redox behavior in the alkaline media, and to develop methods for the separation of non-pertechnetate species from LAW by either their conversion to pertechnetate or direct removal. Moreover, effect of radiolysis on the stability of non-pertechnetate species are critical to evaluate their presence in tank wastes.

The major achievement of this work is the development of stable non-pertechnetate Tc species that are resistant to oxidation to Tc(VII) under conditions of pseudo-Hanford tank supernatant simulant. The key findings are summarized below.

1. Stability of non-pertechnetate generated *ex situ*.
   a. Oxidative stability of the aqua $[Tc(CO)_3(H_2O)_{3-n}(OH)_n]^{1-n}$ ($n = 0 – 3$) compounds is highly dependent on the hydroxide concentration in solution. These species are highly stable in high nitrate solutions at near neutral to mildly alkaline pH. Measurements conducted 1.5 years after sample preparation indicate that they persist in the solution at high fractions (the monitoring of these samples is continuing). In the high salt solutions with high hydroxide concentrations, the $[Tc(CO)_3(H_2O)_{3-n}(OH)_n]^{1-n}$ compounds undergo fast oxidative

decomposition most likely due to the hydrolytic destruction of the Tc-CO backbone via OH^- nucleophilic attack at the carbonyl carbon (Levitskaia et al. 2014).

   b. Oxidative stability of $[Tc(CO)_3]^+$•Ligand complexes was evaluated in a 5 M $NaNO_3$ / 0.1 M NaOH solution and a pseudo-Hanford tank supernatant simulant with about 0.5 M hydroxide concentration. The tested chelators (ligands) included gluconate, IDA, NTA, EDTA, and DTPA. Among these chelators, IDA formed a remarkably stable $[Tc(CO)_3]^+$•IDA complex, so that it accounted for about 70% of total Tc present in the sample at 4 month after sample preparation in both solutions. The re-oxidation rate of the $[Tc(CO)_3]^+$•Gluconate complex was considerably faster, and Tc(I) is completely oxidized to Tc(VII) in about 65 – 70 days. The stability of $[Tc(CO)_3]^+$•Ligand complexes with NTA, EDTA, and DTPA were found to be weak and exist in equilibrium with $[Tc(CO)_3(OH)(H_2O)_2]$ species. In these samples, all $[Tc(CO)_3]^+$ decomposed to Tc(VII) in about 20 days.

2. Stability of non-pertechnetate generated *ex situ*.

   a. Formation and stability of non-pertechnetate generated from TcO_4^- using CO/H_2 reductant at elevated pressure and temperature in pseudo-Hanford tank supernatant simulant with and without gluconate and/or catalytic noble metals was examined. In all samples most TcO_4^- was reduced to non-pertechnetate following this treatment. The reaction products contained liquid and solid fractions. The non-pertechnetate species that formed included Tc in multiple oxidation states. Formation of Tc(I) as $[Tc(CO)_3]^+$ and Tc(VI) compounds in the liquid fractions was observed using ^{99}Tc NMR and EPR methods, respectively. The non-pertechnetate species in the solid fraction was quantified by liquid scintillation counting and preliminarily identified as being Tc(II, IV and/or VI) compounds based on combined NMR/EPR characterization.

   b. It was found that noble metals catalyze reduction of TcO_4^- to $[Tc(CO)_3]^+$. It is evident from the observation that 72 and 11% of Tc(VII) reduced to Tc(I) in the simulant with and without noble metals, respectively (both simulant samples contained no gluconate). The major reduction product in the pseudo-Hanford tank supernatant simulant containing no catalytic metals was insoluble Tc preliminary identified as Tc(IV) solids. Tc(I) persisted in the liquid fraction of these samples for the corresponding time of about 170 and 50 days, respectively. However, Tc(I) oxidation pathway was different depending on the presence or absence of catalytic noble metals. Presence of catalytic metals promoted conversion of Tc(I) to the NMR-inactive Tc(II/IV/VI) species with intermediate oxidation states. Without noble metals, Tc(I) oxidized directly to pertechnetate, Tc(VII).

   c. For the pseudo-Hanford tank supernatant simulant samples that contained the organic chelator gluconate, the nature of the TcO_4^- reduction products was largely dependent on the presence of catalytic metals. Noble metals promoted formation of Tc(I) identified as $[Tc(CO)_3]^+$•Gluconate complexes. This finding supports the conclusion that the catalytic activity of noble metals promotes the reduction of Tc(VII) to Tc(I). Formation of the NMR-inactive Tc(II/IV/VI) species with intermediate oxidation states in both liquid and solid fraction was observed as well. With time $[Tc(CO)_3]^+$•Gluconate slowly converted to the soluble Tc(II/VI) non-pertechnetate species, which in turn gradually oxidized to TcO_4^-. In the simulant containing gluconate without noble metals, TcO_4^- was exclusively reduced to the soluble non-pertechnetate species preliminarily assigned to a Tc(VI)/gluconate complex. For this test condition neither soluble Tc(I) nor any insoluble Tc was found. Only a liquid fraction of pink color was produced upon reaction completion. The Tc(VI)/gluconate non-pertechnetate species are very stable showing the first sign of oxidation to Tc(VII) in about 70 days post sample generation.

d. One year post generation of the samples, variable amounts of *in situ* obtained non-pertechnetate were present in all reacted simulants. Without catalytic metals, the original simulant (composition shown in Table 1) and simulant with gluconate contained the largest fractions of non-pertechnetate species accounting for 54% (insoluble Tc(IV)) and 62% (soluble Tc(VI)/gluconate) of total Tc in the samples, respectively. Reaction products of the pseudo-Hanford tank supernatant simulant containing both gluconate and noble metals were a mixture of soluble Tc(I) as $[Tc(CO)_3]^+$•Gluconate and soluble Tc(VI)/gluconate and possibly small amounts of insoluble Tc(IV). For this test condition the non-pertechnetate Tc accounted for 62% of the total starting Tc. Non-pertechnetate species in the simulant containing noble metals without gluconate were found to be the least stable accounted for about 10% of total Tc in the sample one year after sample generation.

e. Generated *in situ* $[Tc(CO)_3]^+$ and Tc (II, IV, and/or VI) species have shown considerably more resistance towards oxidation to TcO_4^- than previously thought, as a majority of Tc(VI) species reported in literature convert to TcO_4^- within very short times. Our new results suggest that Tc(VI) species may be more important to the redox chemistry of Hanford waste tanks than previously anticipated. However, the mechanism for our newly found Tc(II, IV, and/or VI) stability remains equivocal. Samples which were generated in the presence of noble metals showed an additional spectral signature as compared to those generated in the absence of noble metals demonstrating that noble metals significantly affect the redox chemistry of Tc. Elucidation of redox mechanisms would allow more intelligent design of parameters to trap Tc oxidation states and facilitate more effective methods of separation and storage of the Tc in Hanford tanks. The above studies also highlighted how complex the redox chemistry of Tc is given the large variation in the stability of formed species depending upon the identity and presence of chelators or the noble metals. For this reason we feel that it is important to expand the study to encompass other transition metals besides the noble metals used to date. The Hanford tank waste contains a myriad of other metals that might interact with the Tc redox chemistry.

A key finding of this work is that stability of non-pertechnetate in the in the Hanford tank supernatants may potentially be explained by inter-conversion among Tc species in various oxidation states. The finding that the small organic chelators (e.g., IDA or gluconate) can stabilize Tc(VI) in the supernatants for prolonged times is significant, in particular because this Tc oxidation state is usually regarded as highly unstable. This also can be accentuated by lack of the analytical methods to quantify and characterize Tc(VI). To this end, development of an EPR method is critical to the actual tanks waste analysis.

Results of this project emphasize that considerable work remains, specifically to achieve control over Tc redox behavior in the alkaline media, and to develop methods for the separation of non-pertechnetate species from LAW by either their conversion to pertechnetate or direct removal. Examination of the actual tank waste collected from various Hanford tanks for Tc speciation and feasibility of treatment of total Tc is integral for the development of successful waste processing strategies.

6.0 References

Astheimer L, J Hauck, HJ Schenk, K Schwochau. 1975. "Tetraoxo Anions of Hexavalent Technetium and Rhenium." *J. Chem. Phys*. 63: pp. 1988-1991.

Alberto R, R Schibli, A Egli, U Abram, S Abram, TA Kaden, and PA Schubiger. 1998. “Steps towards $[(C_5Me_5)TcO_3]$: Novel synthesis of $[(C_5Me_5)Tc(CO)_3]$ from $[\{Tc(\mu^3\text{-}OH)(CO)_3\}_4]$ and oxidation of $[(C_5Me_5)M(CO)_3]$ (M = Tc, Re) with Br_2.” *Polyhedron*, 17(7), pp. 1133 1140.

Bernard JG, E Bauer, MP Richards, JB Arterburn, and RM Chamberlin. 2001. “Catalytic reduction of pertechnetate (99TcO4−) in simulated alkaline nuclear wastes.” *Radiochim. Acta* 89, pp. 59–61.

Cho H, WA de Jong, BK McNamara, BM Rapko, and IE Burgeson. 2004. “Temperature and Isotope Substitution Effects on the Structure and NMR Properties of the Pertechnetate Ion in Water.” *J. Am. Chem. Soc*. 126, 11583-11588.

Colton R. 1962. "Technetium Chloride." *Nature* 193: pp. 872-873.

Colton R and IB Tomkins. 1968. "Halides and Oxide Halides of Technetium. I. Technetium (V) Oxide Halides and the Reaction of Thionyl Chloride with Ammonium Pertechnetate." *Aust. J. Chem*. 21, pp. 1981-1985.

Deutsch E, WR Heineman, R Hurst, JC Sullivan, WA Mulac, and S Gordon. 1978. "Production, Detection, and Characterization of Transient Hexavalent Technetium in Aqueous Alkaline Media by Pulse Radiolysis and Very Fast Scan Cyclic Voltammetry." *J. Chem. Soc. Chem. Comm*., pp. 1038-1040.

Duncan JB, SE Kelly, RA Robbins, RD Adams, MA Thorson, and CC Haass. 2011. *Technetium Sorption Media Review*. RPP-RPT-S0122, Rev. 0, Washington River Protection Solutions, LLC, Richland, WA.

Franklin KJ, CJL Lock, BG Sayer, and GJ Schrobilgen. 1982. “Chemical Applications of Technetium-99 NMR Spectroscopy: Preparation of Novel Technetium(VII) Species and Their Characterization by Multinuclear NMR Spectroscopy.” *Journal of the American Chemical Society*, 104(20), pp. 5303-5306.

Gorshkov NI, AA Lumpov, AE Miroslavov, and DN Suglobov. 2000. “Synthesis of $[Tc(CO)_3{}^+\bullet(H_2O)_3]^+$ ion and investigation of its reaction with hydroxyl ion in the aqueous solutions.” *Radiochemistry*, 45(2), pp: 116-119.

Hall GB, SD Chatterjee, TG Levitskaia, T Martin, NA Wall, and ED Walter. 2015. *Synthesis and Characterization of Tc(I) Carbonyl Nitrosyl Species Relevant to the Hanford Tank Waste: FY 2016 Status Report*. PNNL-24916, EMSP-RPT-030, Pacific Northwest National Laboratory, Richland, WA.

Hurst RW. "Part I. Carbon and Mercury-Carbon Optically Transparent Electrodes. Part II. Investigation of Redox Properties of Technetium by Cyclic Voltammetry and Thin Layer Spectroelectrochemistry." Ph.D. dissertation (University of Cincinnati, Cincinnati, Ohio, 1980), 198 pp.

Kissel G and SW Feldberg. 1969. "Disproportionate of the Technetate Ion in Aqueous Alkaline Media. An Electrochemical Study." *J. Phys. Chem.* 73: pp. 3082-3088.

Krychkov SV, AK Pikaev, AF Kuzina, and VI Spitsyn. 1979. "Electrolytic Dissociation of Technetic Acid in Aqueous Solution by Pulsed Radiolysis." *Proc. Acad. Sci. USSR, Phys. Chem. Sect.* (Engl, trans.) 247: pp. 690-692.

Levitskaia TG, A Andersen, SD Chatterjee, GB Hall, ED Walter, and NM Washton. 2015. *Spectroscopic Properties of Tc(I) Tricarbonyl Species Relevant to the Hanford Tank Waste*. PNNL-25000, EMSP-RPT-032, Pacific Northwest National Laboratory, Richland, WA.

Levitskaia TG, A Andersen, SD Chatterjee, HM Cho, JM Peterson, BM Rapko, ED Walter, and NM Washton. 2014. *Speciation and Oxidative Stability of Alkaline Soluble, Non-Pertechnetate Technetium*. PNNL- 23654, EMSP-RPT-024, Pacific Northwest National Laboratory, Richland, WA.

Lukens WW, JJ Bucher, NM Edelstein, and DK Shuh. 2002. "Products of Pertechnetate Radiolysis in Highly Alkaline Solutions: Structure of $TcO_2.xH_2O$." *Environ.Sci. Technol.* 2002, 36, 1124-1129.

Lukens WW, DK Shuh, NC Schroeder, and KR Ashley. 2004. "Identification of the Non-Pertechnetate Species in Hanford Waste Tanks, Tc(I)-Carbonyl Complexes." *Environ. Sci. Technol.*, 38(1), pp. 229-33.

Majumdar SK, RA Pacer and CL Rulfs. 1969. “Rhenium and Technetium (VI) and Meso (VII) Species.” *J. Inorg. Nucl. Chem.*, 31: pp. 33- 41.

Osborne DW, F Schreiner, K Otto, JG Malm, and H. Selig. 1977. "Heat Capacity, Entropy, and Gibbs Energy of Technetium Hexafluoride Between 2.23 and 350 K; Magnetic Anomaly at 3.12 K; Mean β Energy of ^{99}Tc." *J. Chem. Phys.* 68, pp. 1108-1118.

Rapko BM, SA Bryan, JL Bryant, S Chatterjee, MK Edwards, JY Houchin, TJ Janik, TG Levitskaia, JM Peterson, RA Peterson, SI Sinkov, FN Smith, and RS Wittman. 2013a. *Development of a Chemistry-Based, Predictive Method for Determining the Amount of Non-Pertechnetate Technetium in the Hanford Tanks: FY 2012 Progress Report*. PNNL-22173, Pacific Northwest National Laboratory, Richland, WA.

Rapko BM, SA Bryan, S Chatterjee, TG Levitskaia, JM Peterson, RA Peterson, and SI Sinkov. 2013b. *Investigations into the Nature of Alkaline Soluble, Non-Pertechnetate, Technetium*. PNNL-22957, EMSP-RPT-018, Pacific Northwest National Laboratory, Richland, WA.

Rard JA, MH Rand, G Anderegg, and H Wanner. 1999. *Chemical Thermodynamics of Technetium*, edited by M. C. A. Sandino and E. Östhols (North Holland/Elsevier, Amsterdam, 1999).

Rard JA. 1983. *Critical Review of the Chemistry and Thermodynamics of Technetium and Some of Its Inorganic Compounds and Aqueous Species*. Lawrence Livermore National Laboratory, Manuscript, UCRL-53440.

Rard JA, 2005. "Current Status of the Thermodynamic Data for Technetium and Its Compounds and Aqueous Species," *Journal of Nuclear and Radiochemical Sciences*, 6(3): pp. 197-204, 2005.

Scheele RD, DE Kurath, and GN Brown. 2009. *Scale-Up, Production, and Procurement of PEP Simulants*. PNNL-18678, WTP-RPT-204, Rev 0, Pacific Northwest National Laboratory, Richland WA.

Schroeder NC, SD Radzinski, KR Ashley, AP Truong, and PA Sczcepaniak. 1998. "Science and Technology for Disposal of Radioactive Tank Wastes." Schulz WW and Lombardo NJ, Eds.; Plenum Press: New York; pp. 301-320.

Selig K and JG Malm. 1962. "The Vapor-Pressure and Transition Points of $TcCl_6$." *J. Inorg. Nucl. Chem*. 24:pp. 641-644.

Takayama T, Y Kani, T Sekine, H Kudo, and K Yoshihara. 1995. "Formation of nitridotechnetium(VI) u-oxo dimer complexes with EDTA and EDDA." *J. Radioanal. Nucl. Chem.,* 199, 217-227.

Distribution*

U.S. Department of Energy
Office of Environmental Management

NP Machara
SP Schneider

Pacific Northwest National Laboratory
A Andersen
SD Chatterjee
GB Hall
TG Levitskaia
RA Peterson
BM Rapko
RJ Serne
W Um
ED Walter
NM Washton
Information Release (PDF)

*All distribution will be made electronically.

Pacific Northwest
NATIONAL LABORATORY

U.S. DEPARTMENT OF
ENERGY

Proudly Operated by **Battelle** *Since 1965*

902 Battelle Boulevard
P.O. Box 999
Richland, WA 99352
1-888-375-PNNL (7665)

www.pnnl.gov